2015

Temporal endogenous gene expression profiles in response to lipid-mediated transfection

Timothy M. Martin
University of Nebraska Medical Center, timothy.michael.martin@gmail.com

Sarah A. Plautz
University of Nebraska-Lincoln, sarah.plautz@unl.edu

Angela K. Pannier
University of Nebraska-Lincoln, apannier2@unl.edu

Published in *The Journal of Gene Medicine* 17 (2015), pp. 14–32.
DOI: 10.1002/jgm.2821
PMID: 25663588

Submitted 17 November 2014; revised 1 February 2015; accepted 3 February 2015.

Temporal endogenous gene expression profiles in response to lipid-mediated transfection

Timothy M. Martin,[1] Sarah A. Plautz,[2] and Angela K. Pannier[2,3,4]

1 Department of Pharmaceutical Sciences, Durham Research Center II, University of Nebraska-Medical Center, Omaha, NE, USA
2 Department of Biological Systems Engineering, University of Nebraska–Lincoln, Lincoln, NE, USA
3 Center for Nanohybrid Functional Materials, University of Nebraska–Lincoln, Lincoln, NE, USA
4 Mary and Dick Holland Regenerative Medicine Program, University of Nebraska Medical Center, Omaha, NE, USA

Corresponding author — Angela K. Pannier, 231 L.W. Chase Hall, Lincoln, NE 68583-0726, USA; email apannier2@unl.edu

Abstract

Background — Design of efficient nonviral gene delivery systems is limited as a result of the rudimentary understanding of the specific molecules and processes that facilitate DNA transfer.

Methods — Lipoplexes formed with Lipofectamine 2000 (LF2000) and plasmid-encoding green fluorescent protein (GFP) were delivered to the HEK 293T cell line. After treating cells with lipoplexes, HG-U133 Affymetrix microarrays were used to identify endogenous genes differentially expressed between treated and untreated cells (2 h exposure) or between flow-separated transfected cells (GFP+) and treated, untransfected cells (GFP–) at 8, 16 and 24 h after lipoplex treatment. Cell priming studies were conducted using pharmacologic agents to alter endogenous levels of the identified differentially expressed genes to determine effect on transfection levels.

Results — Relative to untreated cells 2 h after lipoplex treatment, only downregulated genes were identified ≥ 30-fold: *ALMS1*, *ITGB1*, *FCGR3A*, *DOCK10* and *ZDDHC13*. Subsequently, relative to GFP– cells, the GFP+ cell population showed at least a five-fold upregulation of *RAP1A* and *PACSIN3* (8 h) or *HSPA6* and *RAP1A* (16 and 24 h). Pharmacologic studies altering endogenous levels for *ALMS1*, *FCGR3A*, and *DOCK10* (involved in filopodia protrusions), *ITGB1* (integrin signaling), *ZDDHC13* (membrane trafficking) and *PACSIN3* (proteolytic shedding of membrane receptors) were able to increase or decrease transgene production.

Conclusions — *RAP1A*, *PACSIN3* and *HSPA6* may help lipoplex-treated cells overcome a transcriptional shutdown due to treatment with lipoplexes and provide new targets for investigating molecular mechanisms of transfection or for enhancing transfection through cell priming or engineering of the nonviral gene delivery system.

Keywords: ALMS1, FCGR3A, GFP, HEK 293T, ITGB1, microarray analysis, nonviral gene delivery, temporal gene expression profile

Introduction

DNA delivery provides a mechanism to directly alter endogenous gene expression and cellular behavior with applications in functional genomics [1], tissue engineering [2], medical devices [3] and gene therapy [4, 5]. Viruses and the profuse knowledge about the molecular mediators of viral infection [6] have been exploited to develop

very efficient viral gene delivery systems [7]. However, oncogenicity, immunogenicity, and the lack of repeated dosing capability [8–11] of viruses have spurred research towards enhancing the efficacy of nonviral DNA carriers. Nonviral carriers such as cationic lipids (i.e. lipoplexes) [12–20] and polymers (i.e. polyplexes) [21] do not have the problems associated with viruses but suffer from low transfection. However, an incomplete understanding of the molecules and mechanisms that facilitate successful nonviral transfection precludes the efficient design of more efficient nonviral systems [19, 22–24].

Towards a better understanding of nonviral transfection, transcriptome profiling has been used to identify the cellular and tissue response after treatment with nonviral gene carriers by comparing treated samples with untreated samples [23, 25–29]. For example, a previous study used microarrays to identify the *in vivo* cellular response to treatment of lipoplexes and found type I interferon to be upregulated in the spleen after treatment of polyethylene glycol-modified lipoplexes as a result of delayed endosomal escape. That study provided a molecular framework to redesign the DNA carrier for improved safety of the lipoplex, informed through comparison of the gene expression profiles of treated tissue to untreated tissue [7]. However, that work was limited in that molecules facilitating transfection were not identified (i.e. no comparison of gene profiles from treated and transfected cells to treated but untransfected cells was made) to provide a molecular basis to redesign the DNA carrier for improved transfection efficiency. Another study used microarrays to highlight the time- and vector-dependence of the gene expression profile of cells treated *in vitro* with lipoplexes, which showed different types of endogenous genes being over- and under-expressed at 8 h (stress-inducible, immune response, antiviral, cellular growth and division), 24h (cellular growth and division, G protein-coupled receptors, heat shock proteins, transcription/translation effectors, proteasome, senescence and cytoskeletal) and 48 h (cellular growth and division, transcription/translation effectors, Golgi-endoplasmic reticulum trafficking, heat shock proteins, DNA repair, cytoskeletal, and motility) [30] after DNA delivery, although, again, in that work, transfected cells were not studied in isolation and therefore the data provide information about cellular response to treatment with lipoplexes but not about mechanisms that facilitate transfection. Gene expression profiling has also been useful in assessing specific genes expressed by epithelial cells *in vitro* to cope with treatment-induced cytotoxicity and apoptosis, highlighting genes such as interleukin-9 receptor (IL-9R), heat shock protein 70 (HSP70) and met proto-oncogene precursor (cMET) upregulated in cells in lipoplex transfection [26]. Together, these previous studies show the usefulness of microarray analysis to identify genes and pathways elicited after treatment of cells or tissues with nonviral gene delivery systems and that the gene expression profile can vary drastically at various time points after treatment with lipoplexes. However, a substantial gap in knowledge remains about molecules and pathways used by cells to overcome the different barriers that occur over time during DNA transfer [21, 31–43].

To identify mechanisms that facilitate transfection (i.e. successful delivery of the transgene), a lipoplex-treated population of cells can be separated into two subpopulations (transfected and untransfected) and, subsequently, their transcriptome can be profiled using microarray analysis. When transfected and untransfected gene expression profiles are compared, the identified differentially expressed genes provide insight into molecules and mechanisms that facilitate transfection [44, 45]. For example, in our previously published study, we showed *RAP1A* and *HSPA6* endogenous genes to be overexpressed in transfected human embryonic epithelial kidney (HEK 293T) cells 24 h after delivery of the GFP transgene using lipoplexes [45] or polyplexes [44], compared to treated but untransfected cells. Subsequently, priming cells for transfection by altering *RAP1A* or *HSPA6* endogenous levels prior to polyplex or lipoplex treatment, respectively, resulted in an up to 2.5-fold increase in transfection [44, 45]. Those studies demonstrated that transfection can be improved by targeting specific molecules that are over- or under-expressed in transfected cells compared to untransfected cells. Although targeting a single barrier or step in DNA transfer often leads to improved transfection [46], it is unlikely that consideration of a single endogenous gene in DNA carrier design will lead to a therapeutically relevant transfection system. Instead, multi-faceted approaches generally lead to improved transfection [47], although the genes and pathways implicated at other, earlier stages of transfection (e.g. internalization, endosomal escape, nuclear localization, nuclear entry) [21, 31–43] remain unidentified and prevent the design of efficient gene delivery systems. Because lipid and polymer DNA carriers have shown promising *in vitro* and *in vivo* transfection [47], the aim of the present study is to identify genes and pathways implicated at these earlier stages for lipid vectors, whereas our other work focuses on polymer vectors [48].

The objective of the present study was to identify endogenous genes differentially expressed at 2, 8, 16 and 24 h after delivery of the GFP transgene to HEK 293T cells using a cationic lipid vector (Lipofectamine 2000; LF2000). Relative to untreated cells, transcriptome profiling of HEK 293T cells at 2 h post-delivery of lipoplexes was used to identify those endogenous genes that may act in response to treatment stress such as toxicity induced by the complex [22] or inherent intracellular defenses against foreign nucleic acids [49]. Relative to GFP– cells, transcriptome

profiling was used to identify those endogenous genes used by transfected cells (GFP+) that may aid in overcoming cellular barriers known to occur during DNA transfer [21, 31–43] at 8, 16 and 24 h post-delivery of lipoplexes. Events that typically take place 8 h after delivery of complexes to the cells include a high rate of endosomal escape [31, 33], unpacking of plasmid DNA (pDNA) from vector [31, 32], some nuclear localization of complexes or pDNA [31, 33–36], very small amounts of nuclear internalization of complexes or pDNA [34, 36, 37] and very little production of transgenic protein [34, 38]. Events that typically take place 16 h after delivery of complexes to the cells include high rate of nuclear localization of complexes or pDNA [34, 36], continued nuclear internalization of complexes or pDNA [21, 34, 36, 37] and continued production of transgenic proteins [34,38]. Events that take place 24 h after delivery of complexes to the cells include the continued nuclear internalization of pDNA [34,36,37,40], the highest synthesis of transgenic proteins [34, 38, 40] and mitosis (including distribution of transgenic proteins and pDNA to daughter cells) [36, 39]. Therefore, the time points chosen for the investigations in the present study were selected to capture several key cellular events that occur throughout the gene delivery process. We also ascertained the potential role of several of the identified genes for their ability to affect transfection by use of pharmacologic activators or inhibitors of the target endogenous gene. The endogenous genes and pathways that facilitate transfection as identified in the present study can be used as targets for increasing transfection through cell priming or for improved DNA carrier design.

Materials and methods

Cell culture and plasmid preparation

HEK 293T cells (ATCC, Manassas, VA, USA) were cultured in T-75 flasks in Dulbecco's modified Eagle's medium containing 4.5 g/l glucose, supplemented with 10% fetal bovine serum, 1mM sodium pyruvate, 100 units/ml of penicillin-streptomycin (all Gibco, Carlsbad, CA, USA) and maintained at 37°C in a humidified 5% CO_2 atmosphere. For seeding, cells were dissociated at confluence with 1mM ethylenediaminetetraacetic acid (EDTA) and viable cells were counted using a hemocytometer and trypan blue dye exclusion assay. Plasmid pEGFP-LUC encodes both the enhanced green fluorescent protein (EGFP) and firefly luciferase protein (LUC) under the direction of a cytomegalovirus promoter (Clontech, Mountain View, CA, USA), and was used for transfection experiments (see below). Plasmid was purified from bacteria culture using Qiagen (Valencia, CA, USA) reagents and stored in Tris–EDTA buffer solution (10mM Tris, 1mM EDTA, pH 7.4) at –20°C.

Transfection and sample isolation for microarray

Cells were seeded at a density of 44.8×10^3 cells/cm^2 into multiple T-75 flasks. After adherence (approximately 18 h after seeding), lipoplexes were formed using LF2000 in accordance with the manufacturer's instructions (Invitrogen, Carlsbad, CA, USA). Briefly, LF2000 transfection reagent diluted in serum-free Opti-MEM media (Invitrogen) was added dropwise to DNA diluted in Opti-MEM at a lipid: DNA ratio of 1.5:1, mixed by gentle pipetting, and incubated at room temperature for 20 min. After forming the lipoplexes, they were delivered to the media above the cells to deliver 0.15 μg/cm^2 of DNA. Those transfection conditions were optimal for high transfection (typically 70–90%) and low cytotoxicity with optimization performed as described previously [45]. The complexes remained in contact with the cells for the duration of each experiment: 2, 8, 16 and 24h. After the incubation period of the lipoplexes at each time point, cells were dissociated using 0.05% Trypsin-EDTA (except only EDTA for the 2-h condition) and suspended in 1X phosphate-buffered saline (PBS) at 2–5 million cells/ml and placed on ice. For the 2-h time point, because very little GFP had been produced, untreated samples were obtained identically, as were the treated samples, except no lipoplexes were delivered to the cells. For the 8-, 16- and 24-h time points, after dissociation, the treated cells were separated into transfected (GFP+) and untransfected (GFP–) pure cell populations using fluorescence activated cell sorting (FACS), as described previously [45]. Briefly, at 8, 16 or 24 h after the addition of complexes, cells were dissociated, counted, and concentrated in 1X PBS and placed on ice, as described above. Flow cytometric analysis was performed using a B-D FACSVantage SE three-laser, high speed cell sorter (University of Nebraska–Lincoln's Center for Biotechnology Flow Cytometry Core Facility) equipped with a 530/15 nm SE laser. A live gate was set on the GFP+ cell population in forward scatter versus side scatter plot to remove cell debris or clumped cells from the sort. A minimum of 2×10^6 cells for each population (GFP+, GFP–) was collected. Cells were collected at each time point on three different days providing the following independent samples (n=3 for each sample): 2 h treated, 2 h untreated, 8 h GFP+, 8 h GFP–, 16 h GFP+, 16 h GFP–, 24h GFP+ and 24 h GFP– (for an overview of the experimental design, see Figure 1). RNA from each sample was then extracted, purified and hybridized to microarrays (see below).

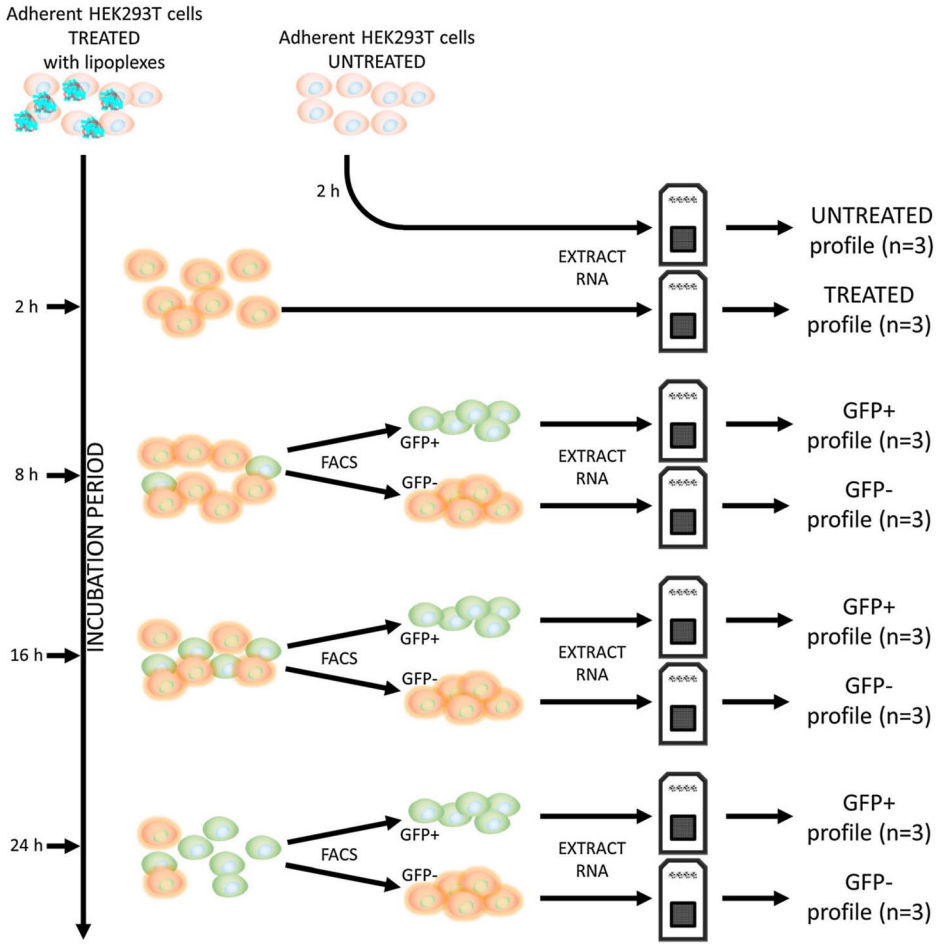

Figure 1. Overview of the experimental design (see Materials and methods). HEK 293T cells were seeded and allowed to become adherent (approximately 18 h). Then, lipoplexes were formed and delivered to adherent cells and allowed to remain in contact for 2, 8, 16 or 24 h. At the 2-h time point, treated cells were harvested and RNA was extracted and hybridized to microarrays. The treated profile was compared with cells that underwent the same treatments, except no lipoplexes were delivered. At the 8-, 16- or 24-h time points, treated cells were FACS separated into GFP positive (GFP+; transfected) and GFP negative (GFP–; untransfected) cell populations and RNA was extracted and hybridized to microarrays. The process was repeated on separate days to achieve n=3 for each population at each time point.

RNA extraction and microarray hybridization

RNA extraction and quality check was performed as described previously [45]. Briefly, after obtaining each sample (24 in total: three each for 2 h treated, 2 h untreated, 8 h GFP+, 8 h GFP–, 16 h GFP+, 16 h GFP–, 24 GFP+ and 24 h GFP–; see also above and Figure 1), total RNA was TRIzol extracted and further purified using a Qiagen RNeasy column (Qiagen) to achieve a 260/280 ratio greater than 1.8 on Nanodrop 2000 (Thermo Scientific, West Palm Beach, FL, USA). After quality assessment using an RNA 6000 Nano LabChip on an Agilent BioAnalyzer 2100 (Agilent Technologies, Santa Clara, CA, USA), purified RNA was reverse transcribed to cDNA and hybridized to Affymetrix GeneChip Human Genome U133 Plus 2.0 Arrays (Affymetrix, Santa Clara, CA, USA) overnight at 45°C, in accordance with the manufacturer's instructions. After streptavidin-phycoerythrin conjugate staining, expression data were read with the GeneChip Scanner 3000 7G (Affymetrix) to obtain the expression data of over 47 000 transcripts and variants annotated for all known genes of the human genome. Affymetrix GeneChip Operating Software (GCOS, version 1.3) was used for washing, scanning and basic data analysis, including calculation of absolute values and normalization of the data with respect to internal standards.

Microarray and bioinformatics analyses

Each microarray provides 11 independent measures of gene expression (n=11) for over 47,000 transcripts and variants annotated for all known genes of the human genome.

Microarray expression data were background adjusted and normalized [50] and quality tested using R/Bioconductor with the AffyCoreTools library package, with all arrays showing good hybridization quality, as described previously [44,45]. The gene expression data has been deposited at the NCBI Gene Expression Omnibus (GEO) accession GSE59666. Differentially expressed genes between treated and untreated (2-h time point) or GFP+ and GFP– (8-, 16- and 24-h time points) were determined using a nonparametric mean-variance smoothing method developed for R programming environment [51]. Microarray data for the 24-h time point were collected previously and analyzed using linear models [45] and were downloaded from GEO accession GSE20615. Those microarrays were again analyzed here, using the nonparametric smoothing method, which resulted in a larger gene set differentially expressed between GFP+ and GFP– gene expression profiles than has been previously reported. Those results are included in the present study, along with the pathways and ontologies enriched to the new gene set (see below). Genes differentially expressed greater than two-fold and posterior probability greater than 0.99 were used for the bioinformatics analysis. Enrichr [52], an open source and freely available gene list enrichment analysis tool, was used to identify enriched pathways for Kyoto Encyclopedia of Genes and Genomes (KEGG) [53], WikiPathways (WIKI) [54], BioCarta [55], protein–protein interacting proteins (PPI Hub Proteins) [56], The Comprehensive Resource of Mammalian Protein Complexes (CORUM) [57], Reactome [58] and Gene Ontology Process (GO) [59]. Each list of differentially expressed genes was uploaded to the Enrichr [52] website and pathways or ontologies enriched greater than a combined score of 5 were reported. The combined score is computed by taking the log of the *p*-value from the Fisher's exact test multiplied by the Z-score of the deviation from the expected rank [52]. Among the differentially expressed genes, the most promising genes that may affect transfection were identified. The genes were selected based on high differential expression, putative gene role and potential to play a role in processes that are known to occur during DNA transfer [21, 31–43], and exploratory gene association network (EGAN) analysis [60]. EGAN analysis was performed as previously described [44] but, briefly, the tool was used to visualize common occurrences among gene–gene interactions and enriched pathways/ontologies [60] and aided in selecting genes to study further (see Supporting information, Figure S1). After identifying target genes, the NextBio [61] Pharmaco Atlas was used to identify pharmacologic agents known to upregulate or downregulate the target gene with a score above 70. Those pharmacologic agents were then used for transfection studies in the presence of pharmacologic agents (see below).

Transfection in the presence of pharmacologic agents

These experiments were performed as previously described to alter the expression of endogenous target genes identified from microarray analysis [45]. The studies acted primarily as a screening tool to confirm whether a particular gene plays an important role in the DNA transfer process. Briefly, transfection studies were performed in the presence and absence of pharmacologic activators or inhibitors of the target genes (selected as described above). HEK 293T cells were seeded in 48-well plates at 44.8×103 cells/cm2 and, 18h later, pharmacologic agents were delivered to the media on the cells to achieve the final desired drug concentration. The pharmacologic agent was allowed to incubate for 1 h, and then lipoplexes were formed (as described above) and delivered to the media above the cells (still containing the pharmacologic agent). The pharmacologic agent and lipoplexes remained in contact with the cells for the next 24 h and then the cells were lysed and transfection levels were quantified by measuring the luciferase activity (relative light units) using the Luciferase Assay System (Promega, Madison, WI, USA) and luminometer (Turner Designs, Sunnyvale, CA, USA), and luciferase activity was normalized to the total protein amount determined with the BCA protein assay (Pierce, Rockford, IL, USA) and compared with transfection levels in vehicle-only control cells. The results were reported as the fold-change to eliminate variability in absolute measures of transfection, respectively, for *ALMS1*, *ITGB1*, *FCGR3A*, *DOCK10*, *PACSIN3* and *ZDDHC13* genes; pharmacologic activators included phenethicillin [62], 1,10-phenanthroline [63], ritonavir [64], nifenazone [62], hydralazine hydrochloride [62], β-acetyl-γ-*O*-hexadecyl-L-α-phosphatidylcholine hydrate (B-AGO-PCL) [65]; and pharmacologic inhibitors included quipazine [62], artemisinine [64,66], gentamicin [64], 8-methoxypsoralen [62], valsartan [64] and nicergoline [62] (all from Sigma- Aldrich, St Louis, MO, USA). The concentrations of the pharmacologic agents selected for the present study were comparable to those tested in the literature showing gene activity [62, 64–66] but were optimized for high transfection and minimal toxicity (not shown) (see Supporting information, Figure S2). Statistical analysis was performed using Prism, version 5 (GraphPad, La Jolla, CA, USA) using Student's *t*-test at a 95% confidence level. Data are reported as the mean±SEM (n=3).

Results

The GFP transgene was delivered to HEK 293T cells using LF2000 transfection reagent. Then, 2 h after delivery of the lipoplexes, the initial cell response was determined

using microarray analysis. Changes in the transcriptome were identified by comparing gene expression profiles of cells treated with lipoplexes with cells not treated by lipoplexes (Figure 1). All genes found to be differentially expressed two-fold or greater are listed in the Supporting information (Table S1). Among the greatest differentially expressed genes in treated cells compared to untreated cells were: *ALMS1*, *ITGB1*, *FCGR3A*, *DOCK10* and *ZDDHC13*, which were downregulated 34.5-, 35.7-, 38.5-, 43.5- and 50.0-fold, respectively (Table 1). Among all genes differentially expressed between treated and untreated cells at the 2-h time point (see Supporting information, Table S1), only *LIMS1* and *ITGB1* were found to be enriched to cellular pathways including cell migration, the inflammatory response, cell adhesion and cell junctions (Table 2). Taken together, treated cells were shown to undergo rapid transcriptional changes in response to treatment with lipoplexes in a highly downregulated manner.

Because most cells internalize lipoplexes within the first few hours of exposure [21,31,33,34,41–43; Sarah A. Plautz (S.A.P) unpublished results] but not all cells actually express the transgene, we next set out to identify those endogenous genes that may facilitate transfection. To do so, lipoplexes were delivered to the cells and, after 8, 16 or 24 h, the treated cell population was sorted into transfected GFP+ and GFP– subpopulations (Figure 1). Using microarray analysis, changes in the transcriptome were identified by comparing GFP+ and GFP– endogenous gene expression

Table 1. Differentially expressed genes comparing treated with untreated gene expression profiles after 2 h of exposure to lipoplexes

Gene	Fold Δ	Name
ALMS1	–34.5	Alstrom syndrome 1
ZDHHC13	–35.7	Zinc finger, DHHC-type containing 13
ITGAL	–37.0	Integrin, alpha L [antigen CD11A (p180), lymphocyte function-associated antigen 1; alpha polypeptide]
AI912723	–38.5	NA
CCDC30	–38.5	Coiled-coil domain containing 30
FCGR3A	–38.5	Fc fragment of IgG, low affinity IIIa, receptor (CD16a)
SLC24A2	–41.7	Solute carrier family 24 (sodium/potassium/calcium exchanger), member 2
CLLU1	–41.7	Chronic lymphocytic leukemia up-regulated 1
ANXA6	–41.7	Annexin A6
ITGB1	–43.5	Integrin, beta 1 (fibronectin receptor, beta polypeptide, antigen CD29 includes MDF2, MSK12)
PER1	–43.5	Period homolog 1 (Drosophila)
TPTE	–45.5	Transmembrane phosphatase with tensin homology
RRM1	–50.0	Ribonucleotide reductase M1
DOCK10	–50.0	Dedicator of cytokinesis 10
BC040304	–55.6	NA
SLC3A1	–62.5	Solute carrier family 3 (cystine, dibasic and neutral amino acid transporters, activator of cystine, dibasic and neutral amino acid transport), member 1
BCL2L10	–83.3	BCL2-like 10 (apoptosis facilitator)

Fold change indicates differential expression of HEK 293T cells transfected with pEGFPLuc/LF2000 microarrays (n=3) compared to untreated microarrays (n=3) with a posterior probability greater than 0.99 at the 2-h time point. Negative numbers indicate downregulation.
NA: not available.

Table 2. Enriched pathways for genes differentially expressed between treated and untreated gene expression profiles after 2 h of exposure to lipoplexes

Source	Term	Score	Genes
KEGG	Leukocyte transendothelial migration (HSA04670)	5.21	***LIMS1, ITGB1***
BioCarta	Local acute inflammatory response (LAIR)	11.84	***LIMS1, ITGB1***
GO	Leukocyte adhesion (GO: 0007159)	7.14	***LIMS1, ITGB1***
GO	Integrin complex (GO: 0008305)	8.26	***LIMS1, ITGB1***
GO	Focal adhesion (GO: 0005925)	7.08	***LIMS1, ITGB1***
GO	Cell-substrate junction (GO: 0030055)	6.69	***LIMS1, ITGB1***
GO	Adherens junction (GO: 0005912)	5.60	***LIMS1, ITGB1***

Genes found in Table 1 and the Supporting information (Table S1) were found to be over-represented to specific terms. The first column indicates the source of pathway database; the second column lists the enriched term; the third column lists the enrichment score; and the last column indicates which of the differentially expressed genes belong to the enriched term. Downregulated genes are shown in italic, and genes greater than five-fold differentially expressed are shown in bold. For a description of the source or score, see Materials and methods.

profiles. All genes found to be differentially expressed two-fold or greater are listed in the Supporting information (Table S1). At the 8-h time point, the greatest differentially expressed genes were *RAP1A* and *PACSIN3*, both upregulated 38.62- or 6.64-fold, respectively (Table 3). At the 16-h time point, the greatest differentially expressed genes were *RAP1A* and *HSPA6*, upregulated 17.30- or 7.42-fold, respectively (Table 3). At the 24-h time point, the greatest differentially expressed genes were once again *RAP1A* and *HSPA6*, upregulated 10.28- or 11.35-fold, respectively (Table 3).

We were next interested in understanding how the gene expression profile changes over time, in terms of the number of genes expressed, as well as which genes were found to be differentially expressed over multiple time points. The number of genes differentially expressed (between GFP+ and GFP–) increased from 8 h to 16 h from seven genes to 27 genes, respectively (Figure 2). *ARMC8*, *ATF3* and *RAP1A* genes were commonly expressed between the two time points (Figure 2). The number of genes differentially expressed decreased from 16 h to 24 h from 27 genes to two genes (Figure 2), respectively, with *HSPA6* and *RAP1A* genes commonly being expressed between the two time points (Figure 2). *RAP1A* showed sustained upregulation in the transfected cell population compared to untransfected cell population at the 8-, 16- and 24-h time points (Figure 2; see also Supporting information, Table S1). The largest number of genes differentially expressed occurred 16 h after exposure to lipoplexes in the transfected cell population.

To determine the role of all differentially expressed genes in transfected cells at each time point (8, 16 and 24 h; see Supporting information, Table S1), we performed a pathway and ontology enrichment analysis (Table 4; see Materials and methods). Pathways enriched from genes differentially expressed at the 8-h time point were the mesenchymal–epithelial transition (MET) and integrin pathways, protein complexes (CLTH, HSPA1A and SMARCA4) and GO processes involved in metabolism, proteolysis and catabolism (Table 4). Pathways enriched at the 16-h time point were spindle and cell cycle pathways, as well as protein complexes involved

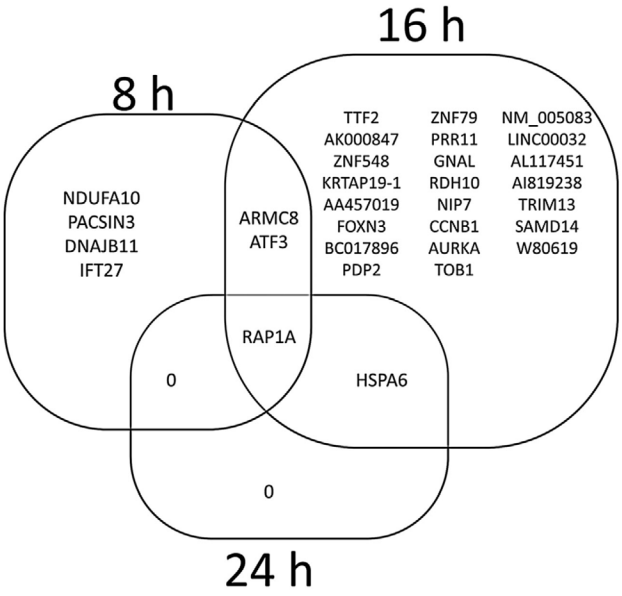

Figure 2. The overlap of genes differentially expressed between the GFP+ and GFP– gene expression profiles is shown for each time point. Data represent genes greater than two-fold differentially expressed comparing transfected microarrays (GFP+; n=3) with treated, untransfected microarrays (GFP–; n=3) with a posterior probability >0.99. The level of differential expression for each gene is provided in the Supporting information (Table S1).

in cell adhesion (RIAM-Rap1-GTP complex), proliferation (CDC2-PCNA-CCNB1-GADD45A complex) and stimuli response (MAPK9) (Table 4). Pathways enriched at the 24-h time point were focal adhesion, migration, MET, integrin and stimuli response (mitogen-activated protein kinase, IL-3, type I interferon, unfolded protein response) pathways, along with protein complexes involved in paracrine signaling (HGFR), GTPase activity, transport (GABARAPL2) and cell adhesion (RIAM-Rap1-GTP complex) (Table 4). Taken together, the pathways and ontologies enriched at each time point may play a role in transfection, and those genes differentially expressed greater than five-fold at each time point may play a significant role in those processes because

Table 3. Temporal cell response after treatment with lipoplexes comparing GFP+ to GFP– gene expression profiles

Time	Gene	Fold	Posterior probability	Accession number	Name
8 h	RAP1A	38.62	1.00	AB051846	RAP1A, member of RAS oncogene family
	PACSIN3	6.64	1.00	AK000847	Protein kinase C and casein kinase substrate in neurons 3
16 h	RAP1A	17.30	1.00	AB051846	RAP1A, member of RAS oncogene family
	HSPA6	7.42	1.00	NM_002155	Heat shock 70-kDa protein 6 (HSP70B′)
24 h	RAP1A	10.28	1.00	AB051846	RAP1A, member of RAS oncogene family
	HSPA6	11.35	1.00	NM_002155	Heat shock 70-kDa protein 6 (HSP70B′)

Comparison of GFP+ to GFP– gene expression levels. Differential expression greater than or less than 1 represents upregulation or downregulation, respectively. Data represent genes differentially expressed comparing transfected microarrays (n=3) with treated, untransfected microarrays (n=3) with a posterior probability greater than 0.99 and differential expression greater than five-fold. The Supporting information (Table S1) lists all genes differentially expressed greater than two-fold.

Table 4. Enriched pathways for genes differentially expressed between GFP+ and GFP– gene expression profiles

Source	Term	Score	Genes
8h			
BioCarta	Mesenchymal-epithelial transition factor (MET) pathway	5.53	**RAP1A**
BioCarta	Integrin pathway	5.43	**RAP1A**
PPI HUB	HSPA1A	14.27	DNAJB11, **PACSIN3, RAP1A**
PPI HUB	SMARCA4	6.80	ATF3, **RAP1A**
CORUM	CLTH (PICALM; phosphatidylinositol binding clathrin assembly protein) complex	8.40	*ARMC8*
GO	Mitochondrial electron transport, NADH to ubiquinone (GO: 0006120)	8.08	NDUFA10
GO	Regulation of proteolysis (GO: 0030162)	7.74	**PACSIN3**
GO	Regulation of protein catabolic process (GO: 0042176)	7.54	**PACSIN3**
16 h			
PPI HUB	MAPK9	5.72	*TOB1*, **RAP1A**, **HSPA6**
CORUM	CDC2-PCNA-CCNB1-GADD45A complex	8.06	*CCNB1*
CORUM	RC complex during G2/M-phase of cell cycle	7.48	*CCNB1*
CORUM	Cell cycle kinase complex CDC2	7.97	*CCNB1*
CORUM	RIAM-Rap1-GTP complex	6.47	**RAP1A**
GO	Spindle (GO: 0005819)	5.03	*AURKA*
24 h			
KEGG	Focal adhesion (HSA04510)	5.57	**RAP1A**
KEGG	Leukocyte transendothelial migration (HSA04670)	5.36	**RAP1A**
KEGG	MAPK signaling pathway (HSA04010)	6.21	**RAP1A**
WIKI	Hepatocyte growth factor receptor signaling (WP313)	5.38	**RAP1A**
WIKI	IL-3 signaling pathway (WP286)	5.36	**RAP1A**
WIKI	Interferon type I (WP585)	5.36	**RAP1A**
BioCarta	MET pathway	5.53	**RAP1A**
BioCarta	Integrin pathway	5.43	**RAP1A**
PPI HUB	GABARAPL2	6.07	**HSPA6**, **RAP1A**
CORUM	RIAM-Rap1-GTP complex (human)	9.17	**RAP1A**
GO	Response to protein stimulus (GO: 0051789)	8.85	**HSPA6**
GO	Response to unfolded protein (GO: 0006986)	8.73	**HSPA6**
GO	Response to biotic stimulus (GO: 0009607)	7.20	**HSPA6**
GO	Response to chemical stimulus (GO: 0042221)	5.11	**HSPA6**
GO	GTPase activity (GO: 0003924)	5.50	**RAP1A**

Selected enriched terms are listed for differentially expressed transcripts comparing GFP+ microarrays to GFP– microarrays at each indicated time point after delivery of pEGFPLuc/LF2000 complexes to HEK 293T cells. The first column indicates the name of pathway database; the second column lists the enriched term; the third column lists the enrichment score; and the last column indicates which of the differentially expressed genes belong to the enriched term. Downregulated genes are shown in italic, upregulated genes are underlined, and genes greater than five-fold differentially expressed are shown in bold. For a description of the source or score, see Materials and methods.

they are highly upregulated: 8 h (*PACSIN3* and *RAP1A*), 16 h (*RAP1A* and *HSPA6*) and 24 h (*RAP1A* and *HSPA6*) (Table 4).

As reported in the present study, microarray analysis revealed genes highly differentially expressed in treated cells compared to untreated cells at the 2-h time point and in GFP+ cells compared to GFP– cells at the 8-, 16- and 24-h time points (Tables 1 and 3). To discriminate whether any of the genes identified in the present study have a potential role in transfection as opposed to genes expressed as a treatment effect, pharmacologic studies were conducted. Those genes highly differentially expressed at the 2-, 8-, 16- or 24-h time points (Tables 1 and 3) were narrowed to a smaller subset to further test based on literature review of each gene's putative function, potential role in the DNA transfer process and exploratory gene association network analysis [60] (see Supporting information, Figure S1; Materials and methods). Highly differentially expressed genes *RAP1A* and *HSPA6* (Table 3) were not studied using pharmacologic agents because we have previously shown that perturbing those genes prior to lipoplex delivery can enhance transfection by up to 2.5-fold [45]. The list of genes was narrowed to *ALMS1*, *ITGB1*, *FCGR3A*, *DOCK10*, *PACSIN3* and *ZDDHC13*. Pharmacologic agents known to activate or inhibit each gene were found using NextBio [61] and from previous studies in the literature [62–66], and were used as a screening tool to confirm whether a particular gene may play an important role in the DNA transfer process. The effect of the pharmacologic agent on transfection levels are summarized in Table 5, with transfection levels provided in Figure 3. In all pharmacologic studies reported here, no cytotoxicity was observed (see Supporting information, Figure S2) with the exception of artemisinin (1mM) and nifenazone (5mM), where minor toxicity was observed (see Supporting information, Figure S2).

When the *ALMS1* gene was activated (phenethicillin) or inhibited (quipazine), prior to delivery of lipoplexes, transfection levels were reduced by 7.6-fold or increased by 1.3-fold, respectively (Figure 3 and Table 5). Similarly, when the

Table 5. Transfection in the presence of pharmacologic agents

Gene	Putative gene function	Pharmacologic agent[a]	Vehicle (Control +)	Transfection fold change[b]
ALMS1	Involved in centriole formation and stability [85] and ciliogenesis [87]	Phenethicillin 10mM ↑ [62]	ddH_2O	*–76****
		Quipazine 1 μM ↓ [62]	ddH_2O	**1.3***
ITGB1	Ubiquitously expressed adhesion antigen [100], which regulates immune cell chemotaxis [101] and inflammatory response after infection [102]. Activation mediates proliferation and inhibits apoptosis [103]	1, 10-Phen 10 μM ↑ [63]	DMSO	**1.3***
		Artemisinine 1mM ↓ [64,66]	$CHCl_3$	*–58****
FCGR3A	FCGR3A transduces signals to cytoplasm, which regulate actin, myosin, membrane fusion and production of reactive oxygen intermediates during phagocytosis of IgG-opsonized particles [93]	Ritonavir 10 μM ↑ [64]	DMSO	**1.3****
		Gentamicin 10mM ↓ [64]	ddH_2O	*–25*
DOCK10	Contains a guanine nucleotide exchange factor domain that activates Rho GTPases with growth promoting and anti-apoptotic function; promotes actin cytoskeleton reorganization [97] and motility via lamellipodia protrusions [98]	Nifenazone 10 μM ↑ [62]	DMSO	**1.3***
		8-methoxy 1 μM ↓ [62]	ddH_2O	*–1.4***
PACSIN3	Involved in proteolytic shedding of ectodomain receptors [115] in dynamin-mediated endocytosis [116] and tubulin nucleation at the centrosome [117]	Hydralazine 1 μM ↑ [62]	ddH_2O	*–13***
		Valsartan 100 μM ↓ [64]	DMSO	**1.5****
ZDDHC13	Palmoylates membrane proteins in Golgi apparatus to regulate membrane-to-membrane trafficking [108] or influence interaction of membrane proteins within lipid rafts [109,110], including Ras GTPases such as RAP1 [109]	B-AGO-PCL 10 μM ↑ [65]	$CHCl_3$	*–11*
		Nicergoline 50 μM ↓ [62]	DMSO	*–19*

a. Effect of pharmacologic agent on gene or protein activity as reported in the literature: ↑, activation; ↓, inhibition.

b. Transfection fold change comparing cells treated with pharmacologic agent with cells treated with vehicle only (Control+) (Figure 3).

Transfection levels were measured 24 h after delivery of complexes to HEK 293T cells. The concentration of the pharmacologic agent was selected forminimal cytotoxicity and maximal effect (see Supporting information, Figure S2). 1,10-Phen, 1,10-Phenanthroline; 8-methoxy, 8-methoxypsoralen; hydralazine, hydralazine hydrochloride; B-AGO-PCL, β-acetyl-γ-O-hexadecyl-L-α-phosphatidylcholine hydrate; ddH_2O, double distilled water; DMSO, dimethyl sulfoxide; $CHCl_3$, chloroform. Data are reported as the mean (n=3) and significant changes between treated and vehicle-only transfection levels are indicated as: * $p<0.05$; ** $p<0.01$; or *** $p<0.001$.

ITGB1 gene was activated (1,10-phenanthroline) or inhibited (artemisinine), transfection levels were increased by 1.3-fold or reduced by 5.8-fold, respectively (Figure 3 and Table 5).When the *FCGR3A* gene was activated (ritonavir) or inhibited (gentamicin), transfection levels were increased by 1.3-fold or decreased by 2.5-fold, respectively (Figure 3 and Table 5). When the *DOCK10* gene was activated (nifenazone) or inhibited (8-methoxypsoralen) transfection levels were increased by 1.3-fold or decreased by 1.4-fold, respectively (Figure 3 and Table 5). When the *PACSIN3* gene was activated (hydralazine) or inhibited (valsartan), transfection levels were decreased by 1.3-fold or increased by 1.5-fold, respectively (Figure 3 and Table 5). When the *ZDDHC13* gene was activated (β-acetyl-γ-*O*-hexadecyl-L-α-phosphatidylcholine hydrate) or inhibited (nicergoline), transfection levels were decreased by 1.1-fold or decreased by 1.9-fold, respectively (Figure 3 and Table 5). Taken together, altering *ALMS1*, *ITGB1*, *FCGR3A*, *DOCK10*, *PACSIN3* or *ZDDHC13* gene activity can affect transfection, showing that microarray analysis can identify genes possibly playing a role in transfection.

The effect of the concentration of the pharmacologic agents on transfection used to activate *ALMS1* or inhibit *ITGB1* or *FCGR3A* was evaluated next (Figure 3) because those agents had the largest impact on transfection. For phenethecillin (*ALMS1* activation), the effect of reduced transfection from the pharmacologic treatment became less apparent as the concentration of the drug decreased: at 10 mM, 100 μM and 1 μM, transfection was reduced by 7.60±0.01-, 1.37±0.14- and 1.17±0.02-fold, respectively (Figure 4). For artemisinine (*ITGB1* inhibition), the effect of reduced transfection from the pharmacologic treatment also became less apparent as the concentration of the drug decreased: at 1 mM, 500 μM, 100 μM and 1 μM, transfection was reduced by 5.78±0.01-, 2.72±0.11-, 1.72±0.04- and 1.19±0.04-fold, respectively (Figure 4). For gentamicin (*FCGR3A* inhibition), the effect of reduced transfection from the pharmacologic treatment became less apparent as the concentration of the drug decreased: at 10mM, 1mM and 10 μM, transfection was reduced by 2.49±0.04-, 1.18±0.12- and 1.15±0.09-fold, respectively (Figure 4).

Discussion

Understanding the intracellular molecules and pathways that may facilitate DNA transfer provides insight into the potential mechanisms required for efficient transfection

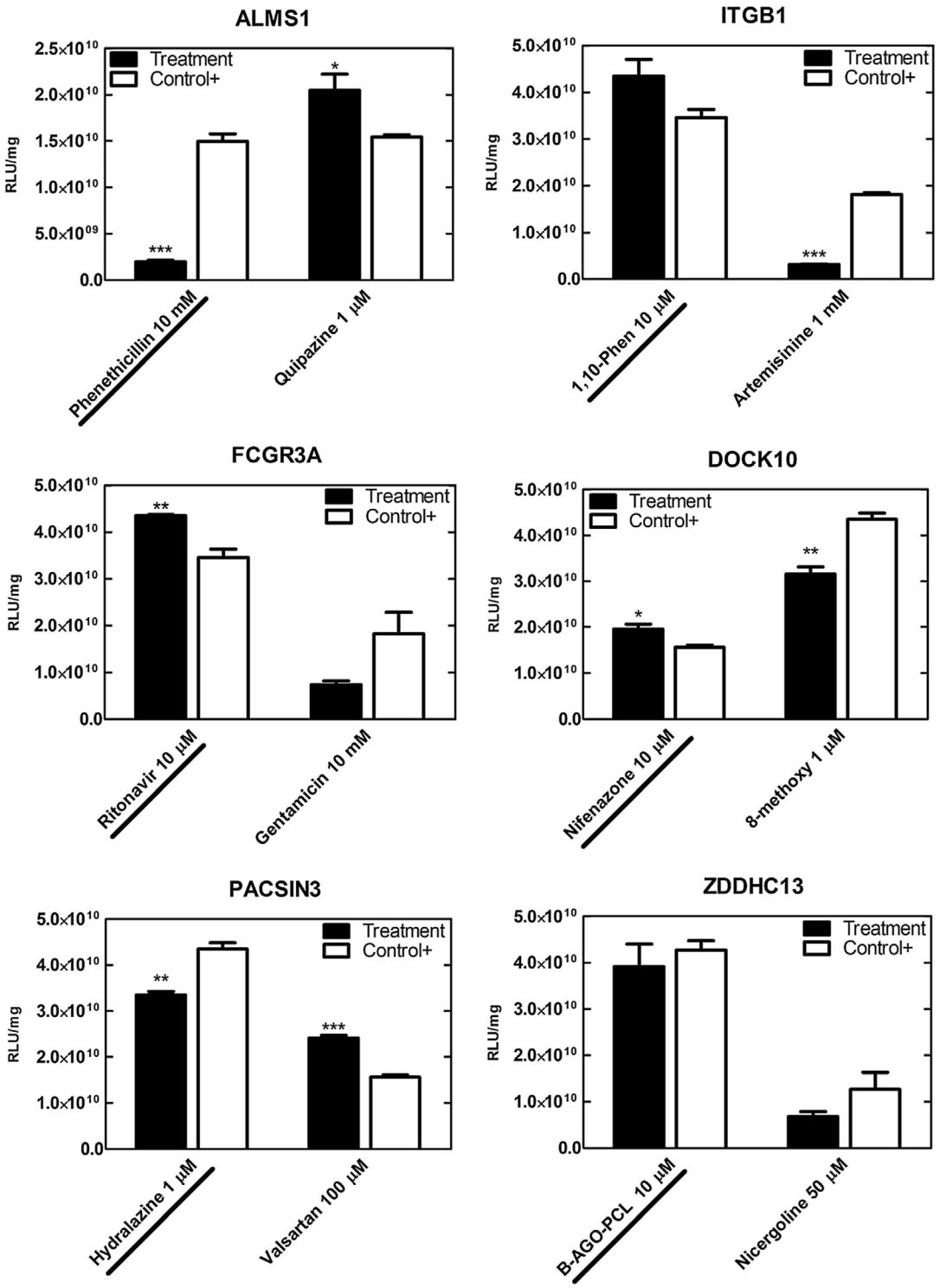

Figure 3. Effect of target gene on transfection for HEK 293T cells treated with indicated pharmacologic agent (black bars) or treated only with vehicle used to deliver the pharmacologic agent (Control+; open bars) (Table 3) to activate (underlined text) or inhibit (plain text) indicated genes. After a 1-h incubation period, lipoplexes were delivered and transfection levels were assayed after 24 h (see Materials and methods). Data are reported as the mean±SEM (n=3) and significant changes between treated and vehicle-only transfection levels are indicated as: * $p<0.05$; ** $p<0.01$; or *** $p<0.001$.

[67], offering targets for designing enhanced nonviral gene delivery systems. Gene transfer requires molecular mediators to actively transfer the delivered DNA [33] through intracellular barriers, into the nucleus [31, 68–76] and for transgene expression [77]. Although the routing kinetics of the lipoplex have been observed as they occur over time

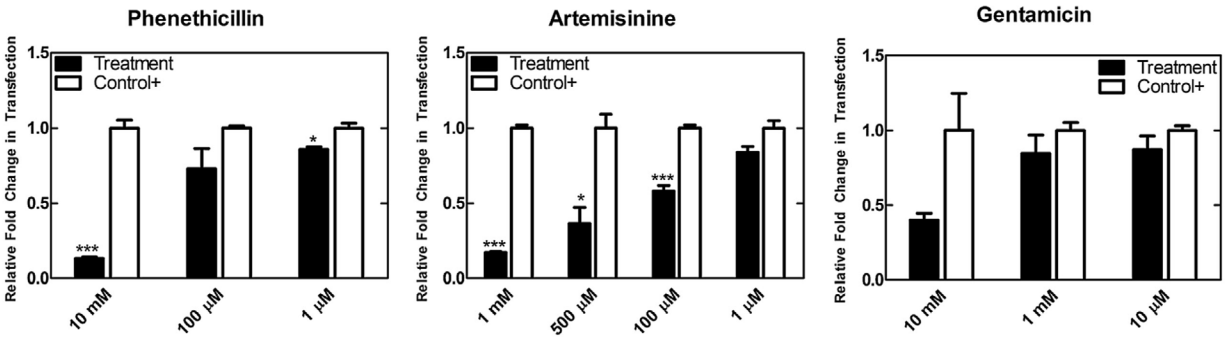

Figure 4. Effect of concentration of pharmacologic on transfection of HEK 293T cells treated with the indicated pharmacologic agent (black bars) or treated only with vehicle used to deliver the pharmacologic agent (Control+; open bars) at a range of concentrations. After a 1-h incubation period, lipoplexes were delivered and transfection levels were assayed after 24 h (see Materials and methods). Data are reported as the mean±SEM (n=3) and significant changes between treated and control+ transfection levels are indicated as: * $p<0.05$ or *** $p<0.001$.

and enable the development of transfection models [34, 40, 46, 78, 79], the molecular mediators used by the cell to route the DNA complex are poorly understood. In the present study, we attempted to fill that gap in knowledge using a transcriptomics approach aimed at identifying molecules and pathways involved in key cellular events known to influence transfection at 2, 8, 16 and 24 h after lipoplex delivery. Because mRNA metabolism and catabolism can be condition- and cell-specific and the mRNA half-life widely varies from approximately 10 min to 10 h or more, our approach may miss the identification of molecules involved in short-lived signaling pathways. To address this challenge of using microarrays and a few selected time points, we integrated the identified endogenous genes and pathways from the present study with other studies that identified short-lived signaling events into a proposed preliminary model of the biology of transfection of HEK 293 T cells by lipoplexes (Figure 5). The endogenous genes and pathways are discussed below in the context of the cellular processes and timing of those processes that occur during DNA transfer.

Treatment of cells with lipoplexes results in a cellular downregulation of transcription

In the present study, gene expression profiles were obtained for HEK 293T cells that were treated with lipoplexes for 2 h compared to untreated cells. Our results show a marked downregulation of 44 genes compared to untreated cells (Table 1; see also the Supporting information, Table S1) affecting cellular pathways in junction, adhesion, migration and inflammation (Figure 5 and Table 2). During this period, the treated cells have been reported to internalize lipoplexes into endosomes and lipoplexes attempt to escape the endosome [22, 34, 40] at the same time as the cell is actively coping with the cytotoxic stress induced by lipoplexes or foreign DNA [80] (Figure 5). Various strategies have been devised to reduce the cytotoxicity, such as maturation time for forming lipoplexes, DNA to liposome ratio, size of lipoplexes and serum-free cell culture conditions [80,81]. However, one recent study advocates a molecular method to reduce cytotoxicity, based on knowing what gene is involved in the toxicity [7] and we advocate the use of a molecular basis to guide the design of improved DNA delivery systems with enhanced transfection [44, 45]. Because all of the genes identified in the present study at the 2-h time point were highly downregulated, the cellular response to exposure of lipoplexes is suggestive of a type of cellular shutdown of transcription, presumably to prevent further cytotoxic assault [22] and further uptake of foreign DNA [80]. We also noted that total RNA was reduced in cells treated with lipoplexes compared to untreated samples (data not shown), providing further evidence for a transcriptional shutdown. The transcriptional shutdown in response to short-term stress is reported to occur in other eukaryotic systems that act to rapidly destabilize mRNAs and coordinate mRNA turnover within a few minutes to achieve a strong activity of stress genes [82]. In the present study, we identified those genes that may play a role in processes that occur in HEK 293T cells after a 2-h exposure to lipoplexes; specifically, *ALMS1*, *ITGB1*, *DOCK10*, *FCGR3A* and *ZDDHC13* genes (Figure 5 and Table 1), which are discussed below in terms of potential hallmarks of the cell shutdown. However, whether the shutdown event is positive or negative for transfection is unclear given the effects of pharmacologic activation of target genes, as discussed below (Table 5 and Figure 3). The results from our studies demonstrate that there are many genes responsible for DNA transfer at different time points and that activating or inhibiting a single gene is unlikely to have a prodigious effect on DNA transfer, agreeing with our pharmacologic studies.

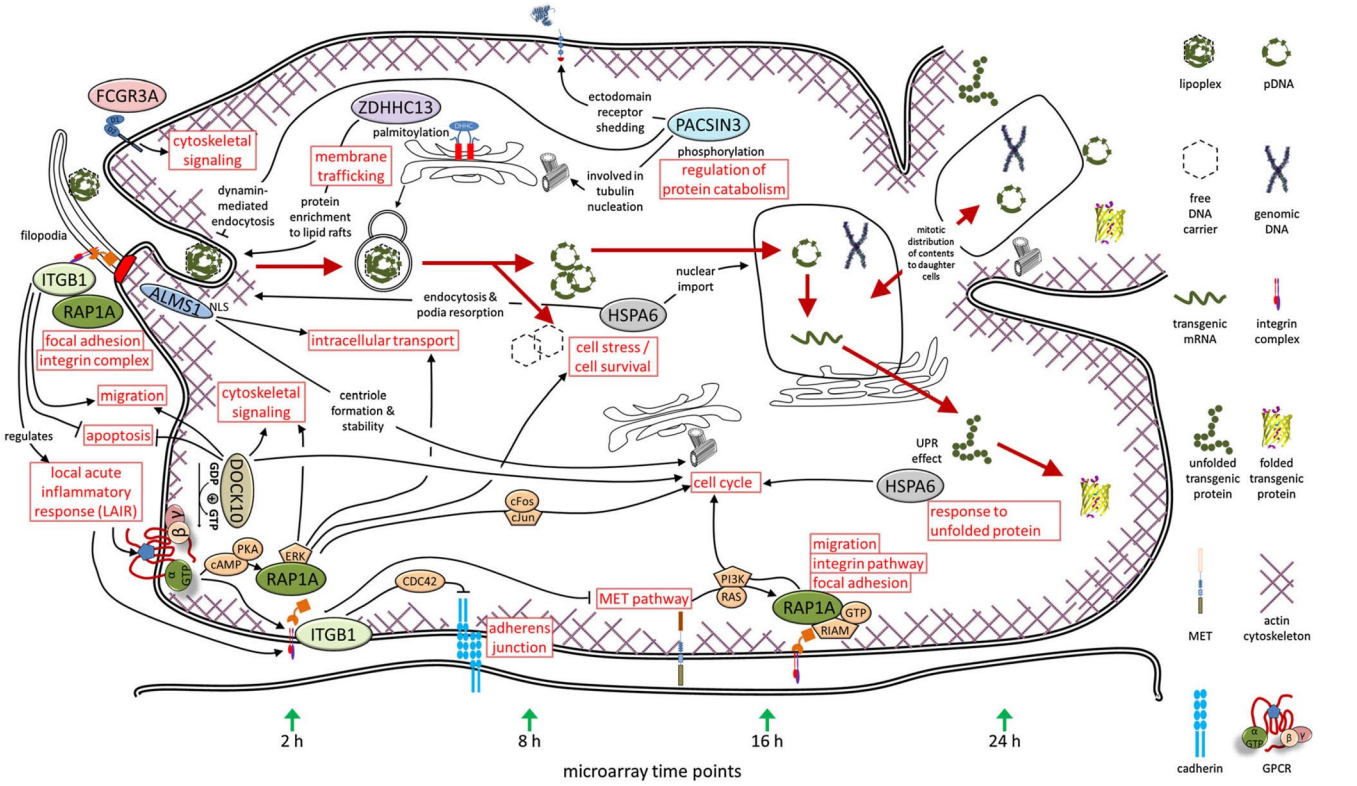

Figure 5. Proposed interaction of genes and pathways during pDNA transfer as identified in the present study. Shown is the outline of a HEK 293T cell with a partial outline of a daughter cell shown in the upper right. The DNA transfer process is shown within the cell, with the initial event of the complex binding to the cell occurring at the far left at time 0 h and subsequent events (large red arrows) occurring over time, from left-to-right. The time points chosen for microarray analysis in the present study are indicated with a green arrow at the bottom and correspond to molecular events shown above the arrow within the cell. Genes, enriched pathways and molecular intermediates as identified or discussed in the present study at each time point appear in the context of the DNA transfer process. Multiple molecular intermediates remain unlisted.

During the first few hours after lipoplex treatment, filopodia have been reported to play a pivotal role in cellular binding and processing of lipoplexes and polyplexes prior to cellular entry via endocytosis [83,84]. Filopodia are slender, actin-rich protrusions that extend outward from the cell body to sense the extracellular environment. Three genes identified in the present study (*ALMS1*, *FCGR3A* and *DOCK10*) are implicated in the generation of such podia protrusions (Figure 5). *ALMS1* is ubiquitously expressed and involved in centriole formation and stability [85], the cell cycle [86] and ciliogenesis [87], and contains two nuclear localization sequences [88], which are all cellular processes or molecules that play a role in transfection [37, 39, 83]. Because the cellular response at 2 h was to downregulate the *ALMS1* gene (Table 1), the cell may be acting in defense as a result of exposure to foreign DNA by preventing the further uptake of lipoplexes via cilia. Hence, we hypothesized that activating *ALMS1* with phenethicillin (penicillin analog) [62] prior to the delivery of lipoplexes would enhance cilia-mediated endocytosis [83, 87] and cell cycle processes [39,86] leading to enhanced transfection. Similarly, we hypothesized that inhibiting *ALSM1* with quipazine (serotonin reuptake inhibitor) [62] prior to lipoplex delivery would lead to decreased transfection. By contrast to our hypothesis, activating *ALMS1* lead to a drastic reduction in transfection (7.6-fold) (Table 5) in a dose-dependent manner (Figure 4), at the same time as inhibiting *ALMS1* slightly increased transfection (1.3-fold) (Table 5). The conflicting result to our hypothesis highlights: (i) that nonspecific pharmacologic agents for *ALMS1* may not be able to adequately test our hypothesis; (ii) that there is a potentially larger role of *ALMS1* beyond transfection because cilia and basal bodies are involved in many inter- and intracellular processes [89,90]; or (iii) that cilia-mediated endocytosis results in an intracellular fate of the lipoplex leading to altered degradation of the lipoplex [91]. In any event, altering *ALMS1* levels may drastically impact transfection.

FCGR3A, also implicated in the generation of podia [92] that have been shown to facilitate endocytosis of lipoplexes [83], was identified as highly downregulated (Table 1) 2 h after exposure of HEK 293T cells to lipoplexes. FCGR3A receptors act to transduce signals to the cytoplasm, which

regulate actin, myosin, membrane fusion and the production of reactive oxygen intermediates during phagocytosis of immunoglobulin (Ig)G-opsonized particles [93] by leukocytes [94]. Although HEK 293T is not a leukocyte cell line, the *FCGR3A* receptor can also be found on embryonic epithelial cells [94] and maintain the necessary cellular machinery for endocytosis without exhibiting respiratory burst [95]. Activation of the receptor can lead to increased proliferation [94] and has been reported to enhance viral infection [96]. Hence, because of those studies and the impact of podia and endocytosis on transfection [83], we hypothesized that activation of *FCGR3A* with the antiretroviral ritonavir [64] would lead to increased endocytosis of lipoplexes and therefore increase transfection. Similarly, we hypothesized that inhibition of *FCGR3A* by gentamicin (aminoglycoside antibiotic) [64] prior to delivery of lipoplexes would lead to reduced transfection. In support of our hypotheses, activating *FCGR3A* increased transfection slightly (1.3-fold) (Table 5) at the same time as inhibiting *FCGR3A* drastically reduced transfection (2.5-fold) (Table 5) in a dose-dependent manner (Figure 4). The distribution of *FCGR3A* receptor in HEK 293T cells should be verified, and the exact mechanisms of *FCGR3A* in transfection of HEK 293T cells remain unclear. However, the results advocate a role of *FCGR3A* in lipoplex-mediated transfection.

DOCK10, also implicated in the generation of podia that have been shown to facilitate endocytosis of lipoplexes [83],was identified as being highly downregulated (Table 1) 2 h after exposure of HEK 293T cells to lipoplexes. *DOCK10* contains a guanine nucleotide exchange factor domain, which activates GTPases (such as *RAP1A* as discussed below) with anti-apoptotic function, promotes actin cytoskeleton reorganization and proliferation [97], and enhances motility via lamellipodia protrusions [98]. Because *DOCK10* function agrees with observations correlated with transfection, such as endocytosis of lipoplexes via podia [83], DNA repair and activation of protein folding chaperones [44,45], cell cycle [39], and cytoskeletal signaling [99], we hypothesized that activation (by nifenazone, a nonsteroidal anti-inflammatory agent) [62] or inhibition (8-methoxypsoralen, a selective inhibitor of DNA synthesis) [62] of *DOCK10* prior to delivery of lipoplexes would lead to enhanced or decreased transfection, respectively. The results reported in the present study support our hypotheses, with activation or inhibition of *DOCK10* enhancing or reducing transfection by 1.3- or 1.4-fold, respectively (Table 5).

Another gene significantly downregulated in cells after 2 h of exposure to lipoplexes was *ITGB1* (Table 1), a ubiquitously expressed adhesion antigen [100], which regulates immune cell chemotaxis [101] and the inflammatory response after infection [102] (Figure 5). Because the activation of *ITGB1* mediates proliferation and inhibits apoptosis [103] and increased cell proliferation is associated with increased transfection [39],we hypothesized that activation (1,10-phenanthroline, uncouples oxidation from phosphorylation in metabolic cycle) [63] or inhibition (artemisinine, an antimalarial drug) [64, 66] of *ITGB1* would increase or decrease transfection, respectively. Indeed, activating *ITGB1* prior to delivery of lipoplexes resulted in a 1.3-fold increased transfection (Table 5), which could be a result of its known effect on proliferative capacity of the cells and therefore increased transfection [39]. Similarly, inhibiting *ITGB1* prior to delivery of lipoplexes resulted in drastically reduced transfection (5.8-fold) (Table 5) in a concentration-dependent manner (Figure 4), which could be a result of the reduced capacity of *ITBG1* to prevent necrosis [102] and toxicity induced by the lipoplex [80], which has been shown to inhibit transgene expression [104]. The ability of *ITGB1* to drastically alter transfection provides evidence that *ITGB1* may be involved in lipoplex-mediated gene delivery and agrees with one study suggesting that lipoplexes electrostatically interact with negative regions of activated β-integrins [105] to piggyback internalization along with the activated integrins. It was advocated that adhesion receptors, in general, serve as natural cell surface receptors for lipoplexes [105] along with other groups showing intercellular cell-adhesion molecule-1, syndecans [106] and integrins [106] to enhance nonviral transfection [107]. Additionally, we advocate a role for integrins in transfection because activating *RAP1A*, involved in integrin-mediated cell adhesion, increases transfection [44,45] (with a role in transfection as discussed below).

ZDDHC13 was identified as another gene significantly downregulated in cells after 2 h of exposure to lipoplexes (Figure 5 and Table 1); *ZDDHC13* serves to palmitoylate membrane proteins in the Golgi apparatus and regulate membrane-to-membrane trafficking [108] or influence the interaction of membrane proteins within lipid rafts [109,110], including Ras GTPases such as *RAP1A* [109]. Because lipid rafts are associated with sites of endocytosis for lipoplexes [111, 112], we hypothesized that activation (B-AGO-PCL, an inflammatory inducer and activator of MAP kinase and MAP kinase kinase) [65] or inhibition (nicergoline, α-adrenergic receptor antagonist and vasodilator) [62] of *ZDDHC13* would lead to increased or decreased transfection, respectively. Activating *ZDDHC13* resulted in a slight 1.1-fold decrease in transfection (Table 5) and did not support our hypothesis, suggesting that activation of *ZDDHC13* may not be directly involved in transfection or that B-AGO-PCL is not suitable for testing our hypothesis. However, inhibiting *ZDDHC13* resulted in a 1.9-fold decrease in transfection (Table 5), which supports our hypothesis suggesting that disrupting the ability of the cell to enrich proteins to lipid rafts would probably lead to reduced endocytosis of lipoplexes and therefore reduced transfection. Increasing the concentration of either pharmacologic agent resulted

in a cytotoxic effect (data not shown), suggesting that *ZDDHC13*-mediated palmitoylation plays a larger role than just membrane trafficking of lipoplexes [113, 114]. The exact mechanism by which transfection is altered by inhibiting *ZDDHC13* remains unknown and requires further investigation, although presumably because of the ability of *ZDDHC13* to affect lipid rafts, the intracellular fate of the lipoplex cargo is also altered, which has been shown to drastically influence transfection [76, 91]. In summary, the activity of endogenous genes and pathways involved in filopodia protrusions (*ALMS1*, *FCGR3A* and *DOCK10*), integrin signaling (*ITGB1*) and membrane trafficking (*ZDDHC13*) may affect transfection early in the DNA transfer process (Figure 5).

Transfected cells overcome cell shutdown and barriers to transfection

As described above, 2 h after lipoplex delivery, all cells exhibited a 'shutdown,' as indicated by the highly downregulated nature of all differentially expressed genes (see Supporting information, Table S1). However, although not all cells eventually express the transgene, some cells do overcome the transcriptional shutdown event and express the transgene. Several cellular processes are known to occur over the course of the next hours (from internalization until transgene expression is detected) (Figure 5), as shown by trafficking studies in the literature [21, 31–40]. What remains unknown are the molecules and pathways that participate in those processes, thereby preventing the rational design of enhanced nonviral gene delivery systems. By comparing gene expression profiles for transfected cells (GFP+) with untransfected cells (GFP–) over a time course of transfection, we were able to identify potential genes that may aid in overcoming barriers to transfection. Specifically, we targeted genes that occur in processes during DNA transfer 8, 16 and 24 h after delivery of lipoplexes, as described below (Figures 1 and 5).

Cellular processes that occur 8 h after exposure of lipoplexes to cells include endosomal escape [31, 33], followed by unpacking of plasmid [31, 32], nuclear localization [31, 33–36], nuclear entry [34,36,37] and a small amount of GFP synthesis [34,38]. By comparing GFP+ and GFP– gene expression profiles, we found *PACSIN3* and *RAP1A* genes to be upregulated at least five-fold, 8 h after exposure to lipoplexes (Figure 5 and Table 3). *PACSIN3* is a gene involved in proteolytic shedding of ectodomain receptors [115], acting to reduce dynamin-mediated endocytosis [116] and involved in tubulin nucleation at the centrosome [117]. Given the gene product function, we hypothesized that activation (hydralazine hydrochloride, an inhibitor of membrane-bound enzymes) [62] or inhibition (valsartan, an angiotensin-receptor blocker) [64] of *PACSIN3* would lead to decreased or increased transfection, respectively. Supporting our hypothesis, activating *PACSIN3* resulted in a 1.3-fold decrease in transfection presumably as a result of decreased endocytosis, which is the primary uptake route of lipoplexes into the cell [91]. Similarly, inhibiting *PACSIN3* resulted in a 1.5-fold increase in transfection, probably a result of enhanced endocytosis of lipoplexes or stabilization of the microtubule network, which may enhance transport of lipoplexes to the cell nucleus [118]. The exact mechanism by which *PACSIN3* affects nonviral transfection remains unclear but, given the processes that occur 8 h after delivery of lipoplexes and the putative function of *PACSIN3*, future studies should be conducted to determine the involvement of *PACSIN3* in endocytosis of lipoplexes, nucleation and modification of the microtubule network, and potential enhancement in nuclear uptake of pDNA.

RAP1A was also overexpressed in the GFP+ to GFP– gene profile comparison after 8, 16 and 24 h of exposure of lipoplexes to the cells (Figure 5 and Table 3). The results suggest that *RAP1A* plays a role in the cellular processes known to occur at those time points: 8 h (endosomal escape [31, 33], followed by unpacking of plasmid [31, 32], nuclear localization [31, 33–36], nuclear entry [34, 36, 37] and a small amount of GFP synthesis [34,38]); 16 h (nuclear localization [34–36], nuclear entry [21, 34, 36, 37] and GFP synthesis [34,38]); and 24 h (2 mitosis [36, 39], high nuclear plasmid number [34, 36, 37, 40] and the highest production of transgene [34,38,40]). *RAP1A* is a small G protein (GTPase) that is activated by guanine nucleotide exchange factors, growth factors, cytokines and many other cell-surface receptors to act as a downstream effector promoting proliferation, cell survival, vesicular trafficking, cytoskeletal organization, integrin-mediated cell adhesion, increased proliferation, focal adhesions and phagocytosis [119, 120]. In our previous work, we found *RAP1A* to be upregulated at the 24-h time point in GFP+ cells relative to GFP– cells and that activating *RAP1A* prior to lipoplex delivery increased transfection two-fold [45], probably affecting cellular processes known to affect transfection such as cell cycle [39], cell survival [80, 102, 104] and endocytosis [111, 112]. In the present study, *RAP1A* continues to show a potential role in nonviral gene delivery because *RAP1A* was overexpressed at 8, 16 and 24 h when using the nonlinear method for calculating differential expression [51] (see Materials and methods). Two potential *RAP1A* activators (*DOCK10* and *ZDDHC13*; see above) and three effectors (*ALMS1*, *FCGR3A* and *ITGB1*) were downregulated 2 h after exposure to lipoplexes. Given the 38.62-fold upregulation of *RAP1A* at the 8-h time point (Table 3), it is possible that the cells able to overcome the transcriptional shutdown and achieve transfection may be those cells that do not exhibit a marked downregulation of *DOCK10* or *ZDDHC13* at the 2-h time point because activating those genes, as described above, would lead to

enhanced transfection. During the 16- and 24-h time points, *RAP1A* could play a role in vesicular trafficking and cytoskeletal organization [119, 120] because activating *RAP1A* acts to acetylate microtubules, which could increase molecular trafficking of lipoplexes to the nucleus, and therefore lead to increased transfection [108]. Additionally, GTPase signaling transduction (e.g. *DOCK10*; see above) via cyclic adenosine monophosphate and protein kinase A can activate *RAP1A*, and protein kinase A has been recently shown to modulate intracellular routing of lipoplexes [121]. Taken together, a potential relationship among expression levels of *RAP1A*activators, *RAP1A* and *RAP1A*-effectors with cellular processes such as focal adhesion, integrin complex, migration, apoptosis, inflammation and cytoskeletal signaling may act together to affect DNA transfer (Figure 5).

HSPA6 was also overexpressed in the GFP+ to GFP– gene profile comparison after 16 and 24 h of exposure of lipoplexes to the cells (Figure 5 and Table 3). The results suggest that *HSPA6* plays a role in the cellular processes noted to occur at those time points [21, 34–40]. *HSPA6*, heat shock 70-kDa protein 6 (HSP70B'), is primarily stress inducible and acts to maintain cell viability [122,123], although *HSPA6* has also been shown to facilitate receptor-mediated endocytosis [124], nuclear import of viral particles [125] and podia resorption [126]. In our previous work using linear models for differential expression determination, we found *HSPA6* to be upregulated at the 24-h time point in GFP+ cells relative to GFP– cells and that activating *HSPA6* prior to lipoplex delivery increased transfection by 2.5-fold [45], probably by altering cellular processes that affect transfection such as nuclear import [125], stabilization of transgene protein folding [122, 123] or podia resorption, which is tied to the cell cycle [126]. In the present study, *HSPA6* continues to show a potential role in nonviral gene delivery because *HSPA6* was overexpressed at 16h and again at 24 h when using the nonlinear method for calculating differential expression [51] (see Materials and methods). Taken together, *HSPA6* may also be involved in nonviral transfection by affecting cellular processes such as cell stress/survival, cell cycle and the response to unfolded protein (Figure 5). In summary, the genes and pathways identified in the present study provide a starting foundation for a preliminary model of the biology of transfection (Figure 5), as well as for future studies to further determine the exact mechanism by which transfection is enhanced.

Conclusions

Identifying those genes and pathways that aid in overcoming barriers to transfection provides targets for engineering enhanced delivery systems and enabling their therapeutic use. In the present study, we began such an endeavor using microarrays to give a temporal and high throughput view of the genes and pathways that occur during DNA transfer when using lipoplexes, and extend our endeavor to polyplexes (in our complementary work) [48]. In the present study, treating cells with lipoplexes showed a transcriptional shutdown of genes involved in cell migration, the inflammatory response, adhesion and cell junctions, which appear to be important to DNA delivery because of their ability to modulate transfection. Possibly more important are the genes and pathways utilized by transfected cells to overcome cellular barriers to transfection. Those genes identified in the present study are involved in metabolism, stimuli response, cell adhesion, proliferation and membrane transport, and are able to modulate transfection. The genes, pathways and pharmacologic agents identified in the present study to alter transfection provide a basis to further explore mechanisms of DNA transfer, prime cells for enhanced transfection from existing DNA delivery strategies and engineer novel nonviral systems that can achieve enhanced transgene expression.

Acknowledgments — Flow cytometry was performed at the Flow Cytometry Core Facility (Dr. Charles A. Kuszynski) and made possible by NIH grant number P20 RR15635 from the COBRE Program of the National Center for Research Resources. Microarray hybridization was performed at the Genomics Core Facility (Dr. Yuannan Xia). All facilities are part of University of Nebraska-Lincoln's Center for Biotechnology (Lincoln, NE, USA). The manuscript was written with contributions from all authors. All authors have given their approval to the final version of the manuscript submitted for publication. Support for this research was provided in part by funds from the National Science Foundation (CBET-1254415), Center for Nanohybrid Functional Materials (NSF EPS-1004094), American Heart Association (#10SDG2640217), the University of Nebraska Foundation (Layman Funds), the Nebraska Research Initiative, University of Nebraska–Lincoln Tobaccos Settlement Funds and USDA CSREES-Nebraska (NEB-21-146 and NEB-26-211). The authors declare that there are no conflicts of interest.

References

1. Pannier AK, Ariazi EA, Bellis AD, Bengali Z, Jordan VC, Shea LD. Bioluminescence imaging for assessment and normalization in transfected cell arrays. *Biotechnol Bioeng* 2007; 98: 486–497.
2. Lu H, Lv L, Dai Y, Wu G, Zhao H, Zhang F. Porous chitosan scaffolds with embedded hyaluronic acid/chitosan/plasmid-DNA nanoparticles encoding TGF-beta1 induce DNA controlled release, transfected chondrocytes, and promoted cell proliferation. *PLoS One* 2013; 8: e69950.
3. Zilberman M, Kraitzer A, Grinberg O, Elsner JJ. Drug-elutingmedical implants. *Handbook Exp Pharmacol* 2010; 197: 299–341.
4. Niidome T, Huang L. Gene therapy progress and prospects: nonviral vectors. *Gene Ther* 2002; 9: 1647–1652.
5. Gao X, Kim KS, Liu D. Nonviral gene delivery: what we know and what is next. *AAPS J* 2007; 9: E92–E104.
6. Dimmock NJ, Easton AJ, Leppard K. *Introduction to Modern Virology* (6th edn). Blackwell Publishing: Malden, MA, 2007.

7. Smith AE, Helenius A. How viruses enter animal cells. *Science* 2004; 304: 237–242.
8. Fasbender A, Marshall J, Moninger TO, Grunst T, Cheng S, Welsh MJ. Effect of co-lipids in enhancing cationic lipid-mediated gene transfer in vitro and in vivo. *Gene Ther* 1997; 4: 716–725.
9. He CX, Tabata Y, Gao JQ. Non-viral gene delivery carrier and its three-dimensional transfection system. *Int J Pharm* 2010; 386: 232–242.
10. Boussif O, Lezoualc'h F, Zanta MA, *et al.* A versatile vector for gene and oligonucleotide transfer into cells in culture and in vivo: polyethylenimine. *Proc Natl Acad Sci U S A* 1995; 92: 7297–7301.
11. Lv H, Zhang S, Wang B, Cui S, Yan J. Toxicity of cationic lipids and cationic polymers in gene delivery. *J Control Release* 2006; 114: 100–109.
12. Susa T, Kato T, Kato Y. Reproducible transfection in the presence of carrier DNA using FuGENE6 and Lipofectamine2000. *Mol Biol Rep* 2008; 35: 313–319.
13. Dalby B, Cates S, Harris A, *et al.* Advanced transfection with Lipofectamine 2000 reagent: primary neurons, siRNA, and high-throughput applications. *Methods* 2004; 33: 95–103.
14. Masotti A, Mossa G, Cametti C, *et al.* Comparison of different commercially available cationic liposome-DNA lipoplexes: Parameters influencing toxicity and transfection efficiency. *Colloids Surf B Biointerfaces* 2009; 68: 136–144.
15. Verma IM, Weitzman MD. Gene therapy: 20-first century medicine. *Annu Rev Biochem* 2005; 74: 711–738.
16. Schaffert D, Wagner E. Gene therapy progress and prospects: Synthetic polymer-based systems. *Gene Ther* 2008; 15: 1131–1138.
17. Tranchant I, Thompson B, Nicolazzi C, Mignet N, Scherman D. Physicochemical optimization of plasmid delivery by cationic lipids. *J Gene Med* 2004; 6(Suppl 1): S24–S35.
18. Ledley FD. Pharmaceutical approach to somatic gene therapy. *Pharm Res* 1996; 13: 1595–1614.
19. Park TG, Jeong JH, Kim SW. Current status of polymeric gene delivery systems. *Adv Drug Deliv Rev* 2006; 58: 467–486.
20. Godbey WT, Wu KK, Hirasaki GJ, Mikos AG. Improved packing of poly (ethylenimine)/DNA complexes increases transfection efficiency. *Gene Ther* 1999; 6: 1380–1388.
21. Godbey WT, Wu KK, Mikos AG. Poly (ethylenimine) and its role in gene delivery. *J Control Release* 1999; 60: 149–160.
22. Godbey WT, Wu KK, Mikos AG. Poly (ethylenimine)-mediated gene delivery affects endothelial cell function and viability. *Biomaterials* 2001; 22: 471–480.
23. Regnstrom K, Ragnarsson EG, Fryknas M, Koping-Hoggard M, Artursson P. Gene expression profiles in mouse lung tissue after administration of two cationic polymers used for nonviral gene delivery. *Pharm Res* 2006; 23: 475–482.
24. Wong SP, Argyros O, Howe SJ, Harbottle RP. Systemic gene transfer of polyethylenimine (PEI)-plasmid DNA complexes to neonatal mice. *J Control Release* 2011; 150: 298–306.
25. Kabanov AV. Polymer genomics: an insight into pharmacology and toxicology of nanomedicines. *Adv Drug Deliv Rev* 2006; 58: 1597–1621.
26. Omidi Y, Hollins AJ, Benboubetra M, Drayton R, Benter IF, Akhtar S. Toxicogenomics of non-viral vectors for gene therapy: A microarray study of lipofectin- and oligofectamine-induced gene expression changes in human epithelial cells. *J Drug Target* 2003; 11: 311–323.
27. Akhtar S, Benter I. Toxicogenomics of non-viral drug delivery systems for RNAi: potential impact on siRNA-mediated gene silencing activity and specificity. *Adv Drug Deliv Rev* 2007; 59: 164–182.
28. Hollins AJ, Omidi Y, Benter IF, Akhtar S. Toxicogenomics of drug delivery systems: exploiting delivery system-induced changes in target gene expression to enhance siRNA activity. *J Drug Target* 2007; 15: 83–88.
29. Brazeau GA, Attia S, Poxon S, Hughes JA. In vitro myotoxicity of selected cationic macromolecules used in non-viral gene delivery. *Pharm Res* 1998; 15: 680–684.
30. Jacobsen L, Calvin S, Lobenhofer E. Transcriptional effects of transfection: the potential for misinterpretation of gene expression data generated from transiently transfected cells. *Biotechniques* 2009; 47: 617–624.
31. Rao NM, Gopal V. Cell biological and biophysical aspects of lipid-mediated gene delivery. *Biosci Rep* 2006; 26: 301–324.
32. Chen BP, Wolfgang CD, Hai T. Analysis of ATF3, a transcription factor induced by physiological stresses and modulated by gadd153/Chop10. *Mol Cell Biol* 1996; 16: 1157–1168.
33. Lai SK, Hida K, Chen C, Hanes J. Characterization of the intracellular dynamics of a non-degradative pathway accessed by polymer nanoparticles. *J Control Release* 2008; 125: 107–111.
34. Varga CM, Hong K, Lauffenburger DA. Quantitative analysis of synthetic gene delivery vector design properties. *Mol Ther* 2001; 4: 438–446.
35. Suh J, Wirtz D, Hanes J. Efficient active transport of gene nanocarriers to the cell nucleus. *Proc Natl Acad Sci U S A* 2003; 100: 3878–3882.
36. Jandt U, Shao S, Wirth M, Zeng AP. Spatiotemporal modelling and analysis of transient gene delivery. *Biotechnol Bioeng* 2011; 108: 2205–2217.
37. Dean DA, Dean BS, Muller S, Smith LC. Sequence requirements for plasmid nuclear import. *Exp Cell Res* 1999; 253: 713–722.
38. Schwake G, Youssef S, Kuhr JT, *et al.* Predictive modelling of non-viral gene transfer. *Biotechnol Bioeng* 2010; 105: 805–813.
39. Brunner S, Sauer T, Carotta S, Cotten M, Saltik M, Wagner E. Cell cycle dependence of gene transfer by lipoplex, polyplex and recombinant adenovirus. *Gene Ther* 2000; 7: 401–407.
40. Varga CM, Tedford NC, Thomas M, Klibanov AM, Griffith LG, Lauffenburger DA. Quantitative comparison of polyethylenimine formulations and adenoviral vectors in terms of intracellular gene delivery processes. *Gene Ther* 2005; 12: 1023–1032.
41. Zelphati O, Szoka FC Jr. Mechanism of oligonucleotide release from cationic liposomes. *Proc Natl Acad Sci U S A* 1996; 93: 11493–11498.
42. Lappalainen K, Miettinen R, Kellokoski J, Jaaskelainen I, Syrjanen S. Intracellular distribution of oligonucleotides delivered by cationic liposomes: Light and electron microscopic study. *J Histochem Cytochem*1997; 45: 265–274.
43. Elouahabi A, Ruysschaert JM. Formation and intracellular trafficking of lipoplexes and polyplexes. *Mol Ther* 2005; 11: 336–347.
44. Martin TM, Plautz SA, Pannier AK. Network analysis of endogenous gene expression profiles after polyethyleneimine-mediated DNA delivery. *J Gene Med* 2013; 15: 142–154.
45. Plautz SA, Boanca G, Riethoven JJ, Pannier AK. Microarray analysis of gene expression profiles in cells transfected with nonviral vectors. *Mol Ther* 2011; 19: 2144–2151.
46. Martin TM, Wysocki BJ, Beyersdorf JP, Wysocki TA, Pannier AK. Integrating mitosis, toxicity, and transgene expression in a telecommunications packet-switched network model of lipoplex-mediated gene delivery. *Biotechnol Bioeng* 2014; 111: 1659–1671.
47. Guo X, Huang L. Recent advances in nonviral vectors for gene delivery. *Acc Chem Res* 2012; 45: 971–979.
48. Martin TM, Plautz SA, Pannier AK. Temporal endogenous gene expression profiles in response to polymer-mediated transfection and profile comparison to lipid-mediated transfection. *J Gene Med* 2015.
49. Cristillo AD, Heximer SP, Forsdyke DR. A 'stealth' approach to inhibition of lymphocyte activation by oligonucleotide complementary to the putative G0/G1 switch regulatory gene G0S30/EGR1/NGFI-A. *DNA Cell Biol* 1996; 15: 561–570.
50. Wu ZJ, Irizarry RA, Gentleman R, Martinez-Murillo F, Spencer F. A model-based background adjustment for oligonucleotide expression arrays. *J Am Stat Assoc* 2004; 99: 909–917.
51. Hu P, Maiti T. A nonparametric mean-variance smoothing method to assess *Arabidopsis* cold stress transcriptional regulator CBF2 overexpression microarray data. *PLoS One* 2011; 6: e19640.
52. Chen EY, Tan CM, Kou Y, *et al.* Enrichr: interactive and collaborative HTML5 gene list enrichment analysis tool. *BMC Bioinformatics* 2013; 14: 128.
53. Kanehisa M, Goto S, Kawashima S, Okuno Y, Hattori M. The KEGG resource for deciphering the genome. *Nucleic Acids Res* 2004; 32(database issue): D277–D280.

54. Kelder T, van Iersel MP, Hanspers K, *et al.* WikiPathways: Building research communities on biological pathways. *Nucleic Acids Res* 2012; 40(database issue): D1301–D1307.
55. Schaefer CF, Anthony K, Krupa S, *et al.* PID: the Pathway Interaction Database. *Nucleic Acids Res* 2009; 37(database issue): D674–D679.
56. Lachmann A, Xu H, Krishnan J, Berger SI, Mazloom AR, Ma'ayan A. ChEA: transcription factor regulation inferred from integrating genome-wide ChIP-X experiments. *Bioinformatics* 2010; 26: 2438–2444.
57. Ruepp A, Waegele B, Lechner M, *et al.* CORUM: the comprehensive resource of mammalian protein complexes – 2009. *Nucleic Acids Res* 2010; 38(database issue): D497–D501.
58. Croft D, O'Kelly G, Wu G, *et al.* Reactome: a database of reactions, pathways and biological processes. *Nucleic Acids Res* 2011; 39(database issue): D691–D697.
59. Ashburner M, Ball CA, Blake JA, *et al.* Gene ontology: tool for the unification of biology. The Gene Ontology Consortium. *Nat Genet* 2000; 25: 25–29.
60. Paquette J, Tokuyasu T. EGAN: exploratory gene association networks. *Bioinformatics* 2010; 26: 285–286.
61. Kupershmidt I, Su QJ, Grewal A, *et al.* Ontology-based meta-analysis of global collections of high-throughput public data. *PLoS One* 2010; 5: 9.
62. Hieronymus H, Lamb J, Ross KN, *et al.* Gene expression signature-based chemical genomic prediction identifies a novel class of HSP90 pathway modulators. *Cancer Cell* 2006; 10: 321–330.
63. Stegmaier K, Ross KN, Colavito SA, O'Malley S, Stockwell BR, Golub TR. Gene expression-based high-throughput screening (GE-HTS) and application to leukemia differentiation. *Nat Genet* 2004; 36: 257–263.
64. Waters M, Stasiewicz S, Merrick BA, *et al.* CEBS – Chemical Effects in Biological Systems: A public data repository integrating study design and toxicity data with microarray and proteomics data. *Nucleic Acids Res* 2008; 36(database issue): D892–D900.
65. Zhu X, Hart R, Chang MS, *et al.* Analysis of the major patterns of B cell gene expression changes in response to short-term stimulation with 33 single ligands. *J Immunol* 2004; 173: 7141–7149.
66. Natsoulis G, Pearson CI, Gollub J, *et al.* The liver pharmacological and xenobiotic gene response repertoire. *Mol Syst Biol* 2008; 4: 175.
67. Horobin RW, Weissig V. A QSAR-modelling perspective on cationic transfection lipids. 1. Predicting efficiency and understanding mechanisms. *J Gene Med* 2005; 7: 1023–1034.
68. Baker AH. Designing gene delivery vectors for cardiovascular gene therapy. *Progr Biophys Mol Biol* 2004; 84: 279–299.
69. Nishikawa M, Huang L. Nonviral vectors in the new millennium: delivery barriers in gene transfer. *Hum Gene Ther* 2001; 12: 861–870.
70. Segura T, Shea LD. Materials for nonviral gene delivery. *Ann Rev Mater Res* 2001; 31: 25–46.
71. Muller OJ, Katus HA, Bekeredjian R. Targeting the heart with gene therapy-optimized gene delivery methods. *Cardiovasc Res* 2007; 73: 453–462.
72. Hagstrom JE. Self-assembling complexes for in vivo gene delivery. *Curr Opin Mol Ther* 2000; 2: 143–149.
73. Azzam T, Domb AJ. Current developments in gene transfection agents. *Curr Drug Deliv* 2004; 1: 165–193.
74. Wiethoff CM, Middaugh CR. Barriers to nonviral gene delivery. *J Pharm Sci* 2003; 92: 203–217.
75. Medina-Kauwe LK, Xie J, Hamm-Alvarez S. Intracellular trafficking of nonviral vectors. *Gene Ther* 2005; 12: 1734–1751.
76. Khalil IA, Kogure K, Akita H, Harashima H. Uptake pathways and subsequent intracellular trafficking in nonviral gene delivery. *Pharmacol Rev* 2006; 58: 32–45.
77. Tachibana R, Ide N, Shinohara Y, Harashima H, Hunt CA, Kiwada H. An assessment of relative transcriptional availability from nonviral vectors. *Int J Pharm* 2004; 270: 315–321.
78. Wysocki BJ, Martin TM, Wysocki TA, Pannier AK. Simulation Supported Estimation of End-to-End Transmission Parameters in Non-Viral Gene Delivery. *IEEE ICC 2014 – Selected Areas in Communications Symposium*, 2014 June; Sydney, New South Wales, Australia (4179–4183).
79. Wysocki BJ, Martin TM, Wysocki TA, Pannier AK. Modelling nonviral gene delivery as a macro-to-nano communication system. *Nano Commun Netw* 2013; 4: 14–22.
80. Dass CR. Cytotoxicity issues pertinent to lipoplex-mediated gene therapy in-vivo. *J Pharm Pharmacol* 2002; 54: 593–601.
81. Hama S, Akita H, Iida S, Mizuguchi H, Harashima H. Quantitative and mechanism-based investigation of post-nuclear delivery events between adenovirus and lipoplex. *Nucleic Acids Res* 2007; 35: 1533–1543.
82. Marguerat S, Lawler K, Brazma A, Bahler J. Contributions of transcription and mRNA decay to gene expression dynamics of fission yeast in response to oxidative stress. *RNA Biol* 2014; 11: 702–714.
83. ur Rehman ZU, Hoekstra D, Zuhorn IS. Mechanism of polyplex- and lipoplex-mediated delivery of nucleic acids: real-time visualization of transient membrane destabilization without endosomal lysis. *ACS Nano* 2013; 7: 3767–3777.
84. ur Rehman Z, Sjollema KA, Kuipers J, Hoekstra D, Zuhorn IS. Nonviral gene delivery vectors use syndecan-dependent transport mechanisms in filopodia to reach the cell surface. *ACS Nano* 2012; 6: 7521–7532.
85. Knorz VJ, Spalluto C, Lessard M, *et al.* Centriolar association of ALMS1 and likely centrosomal functions of the ALMS motif-containing proteins C10orf90 and KIAA1731. *Mol Biol Cell* 2010; 21: 3617–3629.
86. Singla V, Reiter JF. The primary cilium as the cell's antenna: signaling at a sensory organelle. *Science* 2006; 313: 629–633.
87. Hearn T, Spalluto C, Phillips VJ, *et al.* Subcellular localization of ALMS1 supports involvement of centrosome and basal body dysfunction in the pathogenesis of obesity, insulin resistance, and type 2 diabetes. *Diabetes* 2005; 54: 1581–1587.
88. Collin GB, Marshall JD, Ikeda A, *et al.* Mutations in ALMS1 cause obesity, type 2 diabetes and neurosensory degeneration in Alstrom syndrome. *Nat Genet* 2002; 31: 74–78.
89. Gerdes JM, Liu Y, Zaghloul NA, *et al.* Disruption of the basal body compromises proteasomal function and perturbs intracellular Wnt response. *Nat Genet* 2007; 39: 1350–1360.
90. Lee KH, Johmura Y, Yu LR, *et al.* Identification of a novel Wnt5a-CK-1varepsilon- Dvl2-Plk1-mediated primary cilia disassembly pathway. *EMBO J* 2012; 31: 3104–3117.
91. Xiang S, Tong H, Shi Q, Fernandes JC, Jin T, Dai K, Zhang X. Uptake mechanisms of non-viral gene delivery. *J Control Release* 2012; 158: 371–378.
92. Lowry MB, Duchemin AM, Robinson JM, Anderson CL. Functional separation of pseudopod extension and particle internalization during Fc gamma receptor-mediated phagocytosis. *J Exp Med* 1998; 187: 161–176.
93. Swanson JA, Hoppe AD. The coordination of signaling during Fc receptor-mediated phagocytosis. *J Leukoc Biol* 2004; 76: 1093–1103.
94. Fridman WH. Fc receptors and immunoglobulin binding factors. *FASEB J* 1991; 5: 2684–2690.
95. Joiner KA, Fuhrman SA, Miettinen HM, Kasper LH, Mellman I. Toxoplasma gondii: fusion competence of parasitophorous vacuoles in Fc receptor-transfected fibroblasts. *Science* 1990; 249: 641–646.
96. Homsy J, Meyer M, Tateno M, Clarkson S, Levy JA. The Fc and not CD4 receptor mediates antibody enhancement of HIV infection in human cells. *Science* 1989; 244: 1357–1360.
97. Yelo E, Bernardo MV, Gimeno L, Alcaraz-Garcia MJ, Majado MJ, Parrado A. Dock10, a novel CZH protein selectively induced by interleukin-4 in human B lymphocytes. *Mol Immunol* 2008; 45: 3411–3418.
98. Gadea G, Sanz-Moreno V, Self A, Godi A, Marshall CJ. DOCK10-mediated Cdc42 activation is necessary for amoeboid invasion of melanoma cells. *Curr Biol* 2008; 18: 1456–1465.
99. Kasputis T, Pannier AK. The role of surface chemistry-induced cell characteristics on nonviral gene delivery to mouse fibroblasts. *J Biol Eng* 2012; 6: 17.
100. Schmitz B, Park IA, Kaufmann R, Thiele J, Fischer R. Influence of cytokine stimulation (granulocyte macrophage-colony stimulating

factor, interleukin-3 and transforming growth factor-beta-1) on adhesion molecule expression in normal human bone marrow fibroblasts. *Acta Haematol* 1995; 94: 173–181.
101. Kuijpers TW, Mul EP, Blom M, *et al.* Freezing adhesion molecules in a state of high-avidity binding blocks eosinophil migration. *J Exp Med* 1993; 178: 279–284.
102. Ito M, Watanabe M, Ihara T, Kamiya H, Sakurai M. Increased expression of adhesion molecules (CD54, CD29 and CD44) on fibroblasts infected with cytomegalovirus. *Microbiol Immunol* 1995; 39: 129–133.
103. Wang HY, Liu SX, Zhang M. Gene expression profile changes in NB4 cells induced by arsenic trioxide. *Acta Pharmacol Sin* 2003; 24: 646–650.
104. Parker AL, Newman C, Briggs S, Seymour L, Sheridan PJ. Nonviral gene delivery: techniques and implications for molecular medicine. *Exp Rev Mol Med* 2003; 5: 1–15.
105. Zuhorn IS, Kalicharan D, Robillard GT, Hoekstra D. Adhesion receptors mediate efficient non-viral gene delivery. *Mol Ther* 2007; 15: 946–953.
106. Kopatz I, Remy JS, Behr JP. A model for non-viral gene delivery: Through syndecan adhesion molecules and powered by actin. *J Gene Med* 2004; 6: 769–776.
107. Khondee S, Baoum A, Siahaan TJ, Berkland C. Calcium condensed LABLTAT complexes effectively target gene delivery to ICAM-1 expressing cells. *Mol Pharm* 2011; 8: 788–798.
108. Goytain A, Hines RM, Quamme GA. Huntingtin-interacting proteins, HIP14 and HIP14 l, mediate dual functions, palmitoyl acyltransferase and Mg^{2+} transport. *J Biol Chem* 2008; 283: 33365–33374.
109. Linder ME, Deschenes RJ. Palmitoylation: Policing protein stability and traffic. *Nat Rev Mol Cell Biol* 2007; 8: 74–84.
110. Young FB, Butland SL, Sanders SS, Sutton LM, Hayden MR. Putting proteins in their place: Palmitoylation in Huntington disease and other neuropsychiatric diseases. *Prog Neurobiol* 2012; 97: 220–238.
111. Grimmer S, van Deurs B, Sandvig K. Membrane ruffling and macropinocytosis in A431 cells require cholesterol. *J Cell Sci* 2002; 115: 2953–2962.
112. Umeda M, Nojima S, Inoue K. Effect of lipid composition on HVJ-mediated fusion of glycophorin liposomes to erythrocytes. *J Biochem* 1985; 97: 1301–1310.
113. Caron JM. Posttranslational modification of tubulin by palmitoylation: I. In vivo and cell-free studies. *Mol Biol Cell* 1997; 8: 621–636.
114. Touz MC, Conrad JT, Nash TE. A novel palmitoyl acyl transferase controls surface protein palmitoylation and cytotoxicity in *Giardia lamblia. Mol Microbiol* 2005; 58: 999–1011.
115. Mori S, Tanaka M, Nanba D, *et al.* PACSIN3 binds ADAM12/meltrin alpha and up-regulates ectodomain shedding of heparin-binding epidermal growth factor-like growth factor. *J Biol Chem* 2003; 278: 46029–46034.
116. Modregger J, Ritter B, Witter B, Paulsson M, Plomann M. All three PACSIN isoforms bind to endocytic proteins and inhibit endocytosis. *J Cell Sci* 2000; 113: 4511–4521.
117. Grimm-Gunter EM, Milbrandt M, Merkl B, Paulsson M, Plomann M. PACSIN proteins bind tubulin and promote microtubule assembly. *Exp Cell Res* 2008; 314: 1991–2003.
118. Vaughan EE, Geiger RC, Miller AM, *et al.* Microtubule acetylation through HDAC6 inhibition results in increased transfection efficiency. *Mol Ther* 2008; 16: 1841–1847.
119. Bos JL, de Rooij J, Reedquist KA. Rap1 signalling: Adhering to new models. *Nat Rev Mol Cell Biol* 2001; 2: 369–377.
120. Kinbara K, Goldfinger LE, Hansen M, Chou FL, Ginsberg MH. Ras GTPases: Integrins' friends or foes? *Nat Rev Mol Cell Biol* 2003; 4: 767–776.
121. ur Rehman Z, Hoekstra D, Zuhorn IS. Protein kinase A inhibition modulates the intracellular routing of gene delivery vehicles in HeLa cells, leading to productive transfection. *J Control Release* 2011; 156: 76–84.
122. Noonan EJ, Place RF, Giardina C, Hightower LE. Hsp70B' regulation and function. *Cell Stress Chaperones* 2007; 12: 219–229.
123. Noonan E, Giardina C, Hightower L. Hsp70B' and Hsp72 form a complex in stressed human colon cells and each contributes to cytoprotection. *Exp Cell Res* 2008; 314: 2468–2476.
124. Lee SA, Kim BR, Kim BK, *et al.* Heat shock protein-mediated cell penetration and cytosolic delivery of macromolecules by a telomerase-derived peptide vaccine. *Biomaterials* 2013; 34: 7495–7505.
125. Agostini I, Popov S, Li J, Dubrovsky L, Hao T, Bukrinsky M. Heat-shock protein 70 can replace viral protein R of HIV-1 during nuclear import of the viral preintegration complex. *Exp Cell Res* 2000; 259: 398–403.
126. Prodromou NV, Thompson CL, Osborn DP, *et al.* Heat shock induces rapid resorption of primary cilia. *J Cell Sci* 2012; 125: 4297–4305.

Supporting information follows

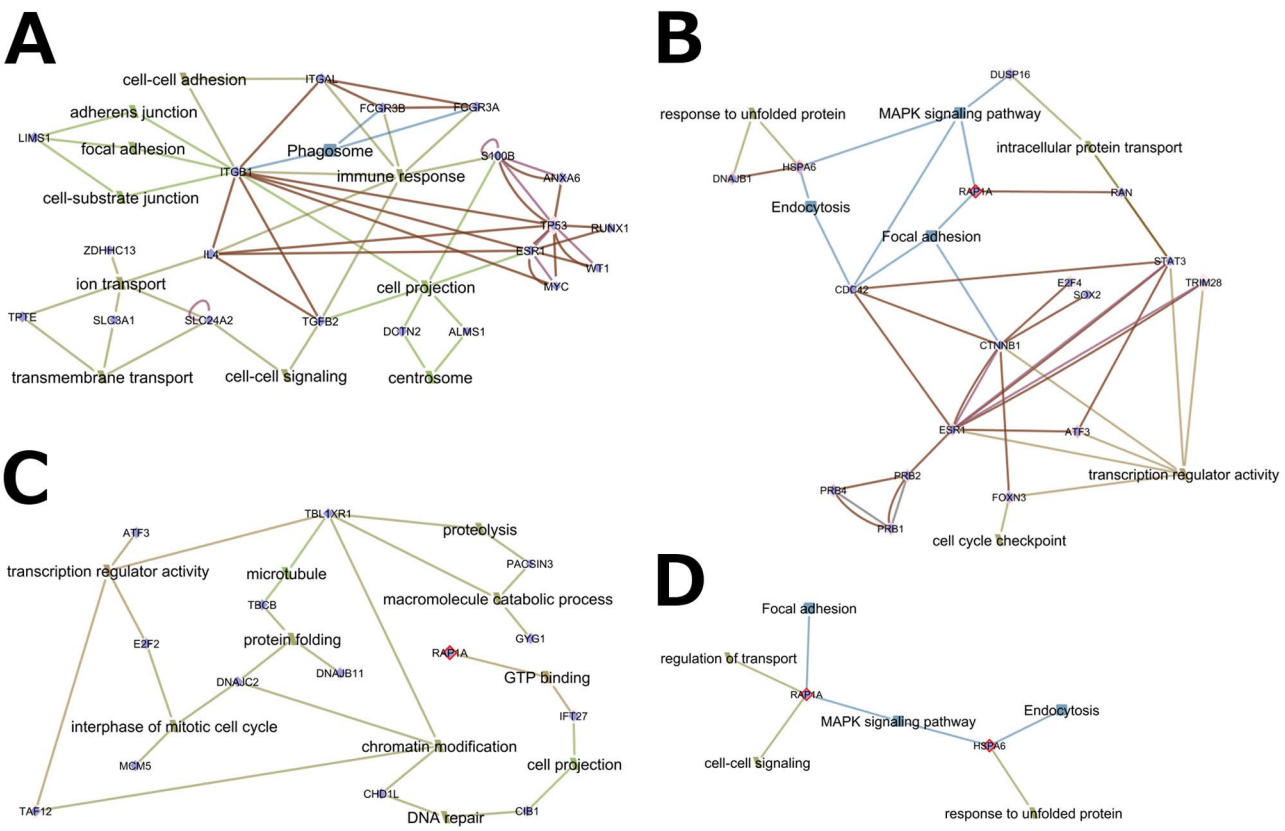

Figure S1. Exploring the interaction among genes and pathways by adding enriched genes and pathways to a network in EGAN to explore and identify candidate genes for a potential role in transfection for the 2-h time point (A), 8-h time point (B), 16-h time point (C) and 24-h time point (D).

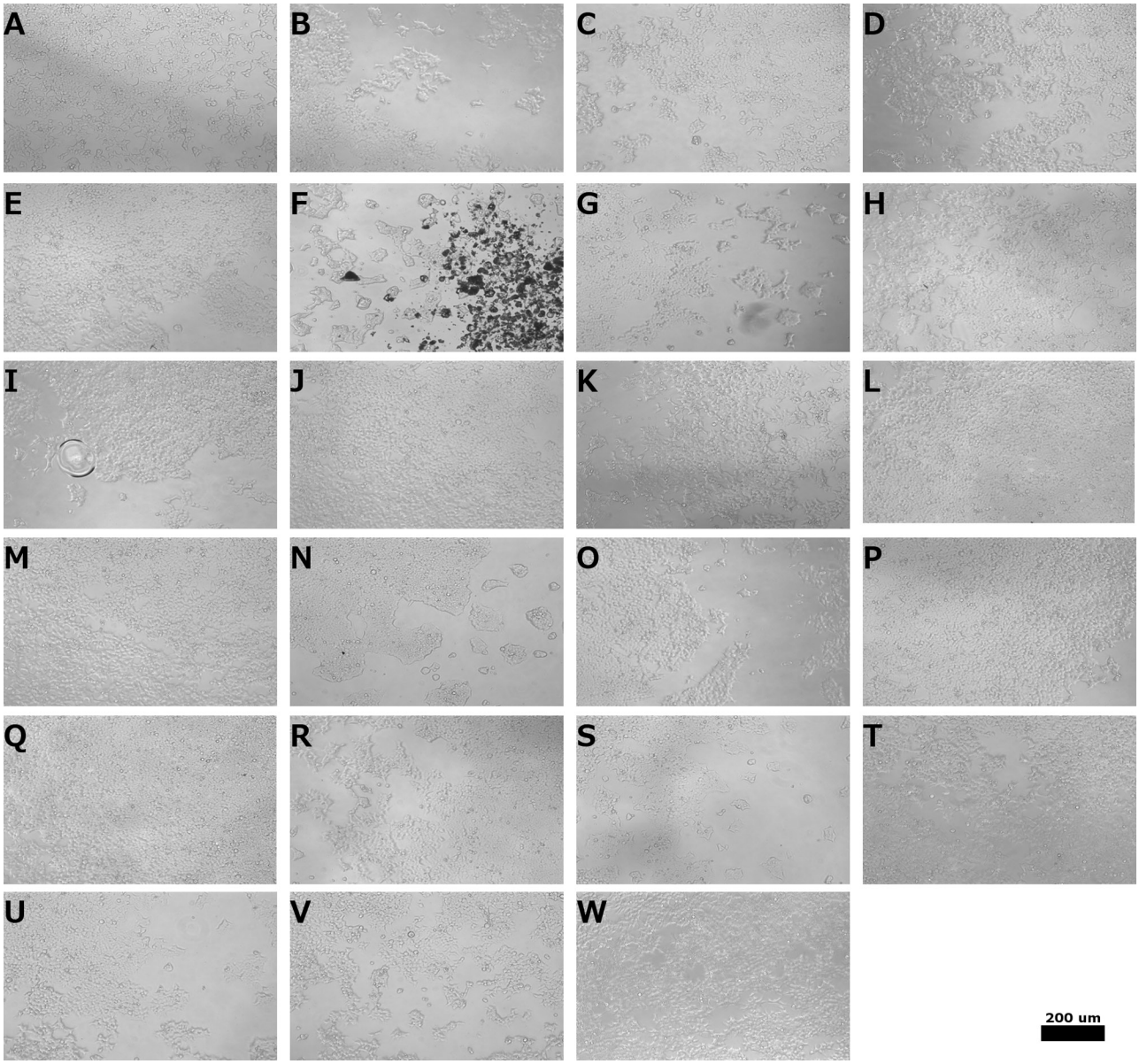

Figure S2. Phase images taken on Leica DMI 3000B (Bannockburn, IL, USA) to assess cell viability and morphology. HEK 293T cells were seeded, allowed to adhere (approximately 18 h); then pharmacologic agent or vehicle control+ was delivered to the media above the cells and after a 1-h incubation, lipoplexes were formed and delivered to the cells. After 24 h, images were taken at ×100 magnification (scale bar is the same for all images and as shown is 200 μM), with representative images shown. (A) Phenethicillin 10mM, (B) phenethicillin 100 μM, (C) phenethicillin 1 μM, (D) quipazine 1 μM, (E) 1,10-phenanthroline 10 μM, (F) artemisinine 1mM, (G) artemisinine 500 μM, (H) artemisinine 100 μM, (I) artemisinine 1 μM, (J) ritonavir 10 μM, (K) gentamicin 10mM, (L) gentamicin 1mM, (M) gentamicin 10 μM, (N) nifenazone 5mM, (O) 8-methoxypsoralen 10 μM, (P) hydralazine hydrochloride 100 μM, (Q) valsartan 100 μM, (R) β-acetyl-γ-*O*-hexadecyl-L-α-phosphatidylcholine hydrate 10 μM, (S) nicergoline 50 μM, (T) ddH2O vehicle control+, (U) CHCL3 vehicle control+, (V) DMSO vehicle control+ and (W) control–. In some cases, when conducting studies using artemisinin at a 1mM concentration (F), some locations in the well showed precipitation of the pharmacologic agent and minor toxicity to the cells. Minor toxicity was also observed when conducting studies using nifenazone at a 5mM concentration (N).

Table S1. Genes differentially expressed greater than two-fold at 2, 8, 16 and 24 h after delivery of lipoplexes.

Time Point	Affy Probe ID	Gene symbol	Gene name	Accession number	Posterior Probability	Differential Expression[1]
2 h	1558501_at	DNM3	dynamin 3	AI631915	0.995	0.478
	1555247_a_at	NA	NA	AF394782	0.990	0.477
	221765_at	UGCG	UDP-glucose ceramide glucosyltransferase	AI378044	0.993	0.465
	33148_at	ZFR	zinc finger RNA binding protein	AI459274	0.993	0.346
	242321_at	PTPN14	protein tyrosine phosphatase, non-receptor type 14	AI628689	0.991	0.346
	235742_at	RHOC	ras homolog family member C	AI436197	0.997	0.276
	235318_at	FBN1	fibrillin 1	AW955612	0.997	0.111
	1555890_at	BC040701	NA	BC040701	0.993	0.110
	231905_at	C20orf96	chromosome 20 open reading frame 96	AL034548	0.998	0.076
	233957_at	AL117426	NA	AL117426	1.000	0.075
	244303_at	AI809906	NA	AI809906	0.995	0.073
	229896_at	GTF2I	general transcription factor IIi	H41907	0.992	0.073
	231482_at	AW274257	NA	AW274257	0.998	0.073
	230574_at	LOC100130938	uncharacterized LOC100130938	AW139393	0.991	0.069
	1565628_at	BM849515	NA	BM849515	0.992	0.068
	1560559_at	AL137539	NA	AL137539	0.993	0.063
	214432_at	ATP1A3	ATPase, Na+/K+ transporting, alpha 3 polypeptide	NM_000703	0.995	0.059
	205666_at	FMO1	flavin containing monooxygenase 1	NM_002021	0.996	0.051
	220450_at	NM_024914	Homo sapiens hypothetical protein FLJ13262 (FLJ13262), mRNA	NM_024914	0.993	0.044
	220550_at	FBXO4	F-box protein 4	NM_018007	0.998	0.042
	241279_at	AV649908	NA	AV649908	0.996	0.040
	1570259_at	LIMS1	LIM and senescent cell antigen-like domains 1	BC015843	0.994	0.040
	1569371_at	LRRC59	leucine rich repeat containing 59	BC033695	0.995	0.038
	214400_at	INSL3	insulin-like 3 (Leydig cell)	AI991694	0.990	0.036
	217558_at	CYP2C9	cytochrome P450, family 2, subfamily C, polypeptide 9	BE971373	0.992	0.035
	237825_x_at	R51853	possible contaminated source	R51853	0.990	0.032
	233788_at	ALMS1	alstrom syndrome 1	AK021679	0.996	0.029
	237999_at	AW195867	NA	AW195867	0.996	0.028
	1554240_a_at	ITGAL	integrin, alpha L (antigen CD11A (p180), lymphocyte function-associated antigen 1; alpha polypeptide)	BC008777	0.991	0.027

	240250_at	AI912723	NA	AI912723	0.991	0.026
	243036_at	CCDC30	coiled-coil domain containing 30	AW364693	0.999	0.026
	204006_s_at	NM_000570	NA	NM_000570	0.994	0.026
	229110_at	SLC24A2	solute carrier family 24 (sodium/potassium/calcium exchanger), member 2	N50083	0.991	0.024
	239244_at	AI806127	NA	AI806127	0.992	0.024
	244250_at	ANXA6	annexin A6	AI917653	0.991	0.024
	1561042_at	ITGB1	integrin, beta 1 (fibronectin receptor, beta polypeptide, antigen CD29 includes MDF2, MSK12)	AF086249	0.996	0.023
	244677_at	AA416756	NA	AA416756	0.996	0.023
	220205_at	TPTE	transmembrane phosphatase with tensin homology	NM_013315	0.997	0.022
	234134_at	AF113689	NA	AF113689	0.996	0.020
	219279_at	DOCK10	dedicator of cytokinesis 10	NM_017718	0.996	0.020
	244436_at	BF829112	NA	BF829112	0.997	0.020
	1556171_a_at	BC040304	NA	BC040304	0.996	0.018
	205800_at	SLC3A1	solute carrier family 3 (cystine, dibasic and neutral amino acid transporters, activator of cystine, dibasic and neutral amino acid transport), member 1	NM_000341	0.991	0.016
	236491_at	BCL2L10	BCL2-like 10 (apoptosis facilitator)	AI813346	0.990	0.012

8 h	Affy Probe ID	Gene symbol	Gene name	Accession number	Posterior Probability	Differential Expression[2]
	1555340_x_at	RAP1A	RAP1A, member of RAS oncogene family	AB051846	1.000	38.623
	222227_at	PACSIN3	protein kinase C and casein kinase substrate in neurons 3	AK000847	1.000	6.641
	205037_at	IFT27	intraflagellar transport 27 homolog (Chlamydomonas)	NM_006860	0.990	3.483
	217860_at	NDUFA10	NADH dehydrogenase (ubiquinone) 1 alpha subcomplex, 10, 42kDa	NM_004544	0.993	3.333
	223054_at	DNAJB11	DnaJ (Hsp40) homolog, subfamily B, member 11	BC001144	0.991	3.025
	202672_s_at	ATF3	activating transcription factor 3	NM_001674	0.999	2.687
	244528_at	ARMC8	armadillo repeat containing 8	AI684748	0.992	0.351

16 h	Affy Probe ID	Gene symbol	Gene name	Accession number	Posterior Probability	Differential Expression[2]
	1555339_at	RAP1A	RAP1A, member of RAS oncogene family	AB051846	1.000	17.297
	213418_at	HSPA6	heat shock 70kDa protein 6 (HSP70B')	NM_002155	1.000	7.417

	1553718_at	ZNF548	zinc finger protein 548	NM_152909	0.997	3.074
	1559291_at	LINC00032	long intergenic non-protein coding RNA 32	AF507950	0.998	2.943
	202672_s_at	ATF3	activating transcription factor 3	NM_001674	0.995	2.856
	222227_at	AK000847	NA	AK000847	0.999	2.806
	214138_at	ZNF79	zinc finger protein 79	AA284829	0.999	2.802
	205021_s_at	FOXN3	forkhead box N3	AA860806	0.993	2.403
	1559995_at	SAMD14	sterile alpha motif domain containing 14	BG911806	0.993	2.233
	206512_at	NM_005083	NA	NM_005083	0.997	2.135
	240789_at	W80619	NA	W80619	0.991	0.493
	1555279_at	ARMC8	armadillo repeat containing 8	BC007934	0.990	0.481
	217659_at	AA457019	NA	AA457019	0.990	0.460
	204092_s_at	AURKA	aurora kinase A	NM_003600	0.996	0.408
	228729_at	CCNB1	cyclin B1	N90191	0.995	0.408
	226021_at	RDH10	retinol dehydrogenase 10 (all-trans)	AW150720	0.994	0.396
	215029_at	AL117451	NA	AL117451	0.994	0.386
	219031_s_at	NIP7	nuclear import 7 homolog (S. cerevisiae)	NM_016101	0.992	0.380
	1569142_at	TRIM13	tripartite motif containing 13	BC029514	0.992	0.376
	232861_at	PDP2	pyruvate dehyrogenase phosphatase catalytic subunit 2	AB037769	0.993	0.366
	1556410_a_at	KRTAP19-1	keratin associated protein 19-1	AJ457067	0.997	0.355
	202704_at	TOB1	transducer of ERBB2, 1	AA675892	0.994	0.349
	228273_at	PRR11	proline rich 11	BG165011	0.992	0.345
	204407_at	TTF2	transcription termination factor, RNA polymerase II	AF080255	0.990	0.345
	206355_at	GNAL	guanine nucleotide binding protein (G protein), alpha activating activity polypeptide, olfactory type	R20102	0.995	0.342
	213931_at	AI819238	NA	AI819238	0.991	0.338
	1569181_x_at	BC017896	NA	BC017896	0.993	0.329
24 h	**Affy Probe ID**	**Gene symbol**	**Gene name**	**Accession number**	**Posterior Probability**	**Differential Expression[2]**
	1555339_at	RAP1A	RAP1A, member of RAS oncogene family	AB051846	1.000	10.28
	213418_at	HSPA6	heat shock 70kDa protein 6 (HSP70B')	NM_002155	1.000	11.35

[1]Differential expression represents comparison of microarray gene expression from cells treated with complexes (n = 3) to microarray gene expression from cells left untreated (n = 3). [2]Differential expression represents comparison of microarray gene expression from cells treated and transfection (GFP+; n = 3) to microarray gene expression from cells treated and untransfected (GFP-; n = 3. Differential expression greater than or less than 1 represents upregulation or downregulation, respectively.